THESIS

ESTIMATING SPATIOTEMPORAL TRENDS IN WILDFIRE SMOKE CONCENTRATIONS IN THE WESTERN UNITED STATES

Submitted by

Katelyn O'Dell

Department of Atmospheric Science

In partial fulfillment of the requirements

For the Degree of Master of Science

Colorado State University

Fort Collins, Colorado

Fall 2018

Master's Committee:

Advisor: Jeffrey R. Pierce
Co-Advisor: Emily V. Fischer

Bonne Ford
Sheryl Magzamen

Copyright by Katelyn O'Dell 2018

All Rights Reserved

ABSTRACT

ESTIMATING SPATIOTEMPORAL TRENDS IN WILDFIRE SMOKE CONCENTRATIONS IN THE WESTERN UNITED STATES

The United States (US) has seen significant improvements in seasonal air quality over the past several decades. However, particulate air quality in summer over the majority of the western US has seen little improvement in recent decades. Particulate matter with diameters < 2.5 microns ($PM_{2.5}$) is a large component of ambient air quality that is associated with negative health effects and visibility degradation. Wildfires are a major summer source of $PM_{2.5}$ in the western US. While anthropogenic-related sources of $PM_{2.5}$ have decreased across the US, wildfires have increased in both frequency and burn area since the 1980s. It is currently uncertain how this increase in wildfires has impacted seasonal air quality trends and how the health effects of wildfire-emitted $PM_{2.5}$ may differ from anthropogenic-sourced $PM_{2.5}$. We do not directly address the latter uncertainty, but rather focus on improving smoke-exposure estimates, which are a critical, yet challenging, component to understanding the health effects of wildfire-emitted $PM_{2.5}$.

In this thesis, we use a combination of satellite estimates, surface observations, and chemical transport models to distinguish wildfire smoke $PM_{2.5}$ from non-wildfire-smoke $PM_{2.5}$ during the summer in the US. We update the record of seasonal trends in $PM_{2.5}$ observed at surface monitors and provide the first estimates of trends in wildfire smoke-specific $PM_{2.5}$. We find continued decreases in total-$PM_{2.5}$ in most seasons and regions of the US. In the summer in

heavily fire-impacted regions of the western US, we find non-decreasing total-$PM_{2.5}$ while wildfire smoke-specific $PM_{2.5}$ has increased and non-wildfire-smoke $PM_{2.5}$ has decreased.

We test the application of blended smoke exposure models, which use multiple data sources as input variables (e.g. satellite-derived aerosol optical depth, chemical transport models, etc.), across the full western US. We incorporate a novel dataset into the model, Facebook posts, which have been shown to correlate well with surface $PM_{2.5}$ concentrations during the western US wildfire season. We find the blended smoke exposure model performs well across the western US (R^2 = 0.66). However, the Facebook dataset is well correlated with interpolated surface monitors (another input variable) and thus does not significantly improve blended smoke-exposure estimates in the western US.

ACKNOWLEDGEMENTS

I thank my advisors: Dr. Jeff Pierce and Dr. Emily Fischer, as well as my committee: Dr. Sheryl Magzamen and Dr. Bonne Ford for their guidance throughout this work. I thank the Pierce and Fischer group members, past and present, (Ali, Anna, Brittany, Emily, Ilana, Jack, Jakob, Jared, Julieta, Steve, Will, and Zitely) for helpful research discussions and for making the second floor a great place to work. I thank my family and friends for their encouragement, love, and support throughout my academic career.

Finally, I would like to thank my grandmother, Nancy, for her constant love and support, and for her encouraging advice: “You can be anything you want to be, and do anything you want to do, as long as you walk with God and keep love in your heart.”

Funding for this work was provided by NASA project number NNX15AG35G.

TABLE OF CONTENTS

1. INTRODUCTION

Ambient air pollution has been identified as one of the top causes of premature mortality worldwide, estimated to have led to 3 million premature deaths in 2010 (OECD, 2016). This threat to human health posed by air pollution is expected to double, or even triple, by the year 2060 (OECD, 2016). Particulate matter, specifically particles with diameters smaller than 2.5 microns ($PM_{2.5}$), is a major component of ambient air pollution and is associated with significant negative health effects (e.g. Dockery et al., 1993; Xing et al., 2016). In the US, over 20% of primary $PM_{2.5}$ emissions are produced by wildland fires (US EPA NEI 2011) .

Unlike most anthropogenic emissions, wildfires are an episodic source of $PM_{2.5}$. In the western US, most wildfire emissions occur in the summer, and occurrence of wildfires varies greatly from year to year. In this region, the interannual variability in wildfire occurrence drives interannual variability in summer aerosol concentrations (Jaffe et al., 2008; Spracklen et al., 2007). Despite their episodic nature and high interannual variability, wildfires can have significant negative impacts on air quality and public health in the western US, especially in high fire years (Gan et al., 2017; Reid et al., 2016).

On decadal timescales, wildfires in the western US have been increasing in frequency and burn area since the mid-1980s (A. L. Westerling et al., 2006). These increases are largely the result of changing climatic factors, in part driven by anthropogenic climate change, including earlier spring snowmelt, warmer temperatures, and reduced winter precipitation (Abatzoglou & Williams, 2016; Pechony & Shindell, 2010; A. L. Westerling et al., 2006). Increases in human-

ignited fires have also had a significant contribution (Balch et al., 2017; Anthony LeRoy Westerling, 2016). Climate and ignition changes have led to approximately 20 additional large wildfires (over 140% increase) and an additional 123,000 ha in burn area (390% increase) over each subsequent decade since the 1973-1982 decade (Westerling, 2016). The most rapid increases in wildfire frequency and burn area over the past two decades have been observed in Pacific Northwest forests (Westerling, 2016). Climate-related increases in wildfire burn area and the number of large fires are projected to continue to increase (Barbero et al., 2015; Spracklen et al., 2009; Yue et al., 2013). Spracklen et al. (2009) project a 54% increase in burn area across the western US and 78% increase specifically in the Pacific Northwest between 2009 and 2050.

As wildfires in the western US increase in frequency and burn area over the next century, emissions of $PM_{2.5}$ from fires are also expected to increase (Ford et al., 2018; Liu et al., 2016; Val Martin et al., 2015). Liu et al. (2016) project 57% and 31% increases in the frequency and intensity, respectively, of smoke events ($\geq$ 2 consecutive days of smoke-elevated $PM_{2.5}$) in the western US by the mid-21st century. It is estimated that by the end of the century, fire-related $PM_{2.5}$ will increase by 55% (Ford et al., 2018) and dominate summertime $PM_{2.5}$ concentrations in the West (val Martin et al. 2015). Similar increases are projected for organic aerosol (Ford et al., 2018; Hallar et al., 2017; Yue et al., 2013). Yue et al. (2013) estimate a 46-70% increase in summertime organic carbon and 20-27% increase in summertime black carbon in the western US by the mid-21st century due to increased wildfire emissions.

Over the past several decades, aerosol concentrations have been decreasing across the eastern US (Hand et al., 2011; Leibensperger et al., 2012; Murphy et al., 2011; Schichtel et al., 2001). Using

sites from the Interagency Monitoring of Protected Visual Environments (IMPROVE) monitor network, Hand et al. (2011) report statistically significant decreases in $PM_{2.5}$ concentrations between 1989 and 2008 at many US monitoring sites, predominantly in the eastern US. Murphy et al. (2011) similarly observed > 25% decrease in annual national-average elemental carbon and fine particle mass concentrations between 1990 and 2004 using the IMPROVE network. Leibensperger et al. (2012) found a 50% (34%) and 27% (16%) US-average decrease in black carbon (organic carbon) using surface observations and the GEOS-Chem model, respectively, over the period 1990-2009. These decreases, which were underpredicted by the GEOS-Chem model, have been linked to large reductions in anthropogenic combustion emissions using both observations and models (Leibensperger et al., 2012; Murphy et al., 2011). Recent work has focused on largely unexpected reductions in organic aerosol in the eastern US (Malm et al., 2017; Ridley et al., 2018). Malm et al. (2017) reported that sulfate and organic aerosol declined concurrently in most of the eastern US between 2001 and 2015. These declines in organic aerosol are the result of reductions in anthropogenic emissions driving changes in secondary organic aerosol chemistry. Up to two-thirds of the drop in annual median organic aerosol concentration can be explained by reductions in vehicle and residential fuel burning emissions (Ridley et al., 2018).

In contrast to the eastern US, changes to western US $PM_{2.5}$ concentrations have been small and largely insignificant (Hand et al., 2011; Murphy et al., 2011). Hand et al. (2011) found a significant decline in summer $PM_{2.5}$ at a few western US sites, however at most western US sites there was an insignificant change in summer $PM_{2.5}$ over the period 1989 to 2008. There were several positive trends observed at remote sites in Montana, Idaho, and Wyoming (Hand et al.,

2011). Murphy et al. (2011) observed positive trends in summer $PM_{2.5}$ at remote sites in Northern California, Colorado, Montana, Wyoming and Utah between 1990 and 2004. Previous work has proposed these positive trends in summer $PM_{2.5}$ in the western US may be due to the influence of wildfires. Extreme $PM_{2.5}$ events (the 98th quantile of daily $PM_{2.5}$ concentrations), attributable to wildfires, have been increasing over the early 21st century in wildfire-prone regions of the western US (McClure & Jaffe, 2018).

While the health impacts of anthropogenic-sourced $PM_{2.5}$ are well understood, the health impacts of wildfire-sourced $PM_{2.5}$ are less certain (Paglione et al., 2014; Reid et al., 2016). Research on the health impacts from wildfire-sourced $PM_{2.5}$ relies heavily on accurate estimates of $PM_{2.5}$ concentrations in smoke plumes. Obtaining $PM_{2.5}$ concentrations within wildfire smoke plumes for exposure estimates is challenging due to the transient nature of the smoke (Brey et al., 2018; Val Martin et al., 2013). In previous epidemiological studies that have estimated the health effects of exposure to wildfire-smoke $PM_{2.5}$, concentrations were estimated by direct measurement of $PM_{2.5}$ by a sparse network of in situ surface monitors, aerosol optical depth (AOD) of the atmospheric column from satellite observations, or surface $PM_{2.5}$ estimates from chemical transport models (CTMs). There have been several case studies that have relied solely on one data source, examples include: satellite data (Rappold et al., 2011), in situ monitors (Elliott et al., 2013), or model simulations (Alman et al., 2016). There are a limited number of studies that have combined several of these datasets to estimate $PM_{2.5}$ concentrations from fires in the western U.S. and those that exist only assess the blended estimates on a small scale (e.g. an individual state) (Lassman et al., 2017; Reid et al., 2016).

Researchers in several geo-science subfields have begun to investigate the potential of using user-generated information (e.g. social media posts) to understand the spatial distribution of natural hazards including fires and associated poor air quality (e.g. Abel et al., 2012; Bedo et al., 2015; De Longueville et al., 2009; Kent & Jr, 2013; Sachdeva et al., 2017; Sachdeva & McCaffrey, 2018; Ford et al., 2017). Ford et al. (2017) show de-identified, aggregated Facebook posts related to air quality and/or wildfire smoke are well correlated with large changes in local $PM_{2.5}$ concentrations during the western US wildfire season. Facebook posts may provide information on the air quality that a population is actually exposed to and thus can be a useful exposure-assessment tool in the US. This unique dataset has the potential to add new information to a data blend of more traditional exposure estimation tools (e.g. surface observations, satellite AOD, CTM simulations) and improve smoke-exposure estimates across the western US.

In this work, we address two major questions regarding the impact of wildfires on seasonal air quality and public health:

1. What fraction of summer $PM_{2.5}$ is attributable to wildfire smoke, and how is that fraction changing in fire-impacted regions as wildfire occurrence increases? (Chapter 2)
2. Can we improve blended smoke-exposure estimates with the addition of user-generated information, and how do these blended exposure models perform across the entire western US? (Chapter 3)

2. THE CONTRIBUTION OF WILDFIRE SMOKE TO US $PM_{2.5}$ AND ITS INFLUENCE ON RECENT TRENDS

2.1. Methods

2.1.1. Time Period and Domain

We investigate changes in continuous US seasonal-mean $PM_{2.5}$ over an 11-year period (2006-2016). This time period is constrained on both ends by data availability, discussed in the following sections. For calculations of seasonal-mean values, we define seasons as follows; winter: January, February, March (JFM); spring: April, May, June (AMJ); summer: July, August, September (JAS); and fall: October, November, December (OND). This choice of months groups the three most active wildfire months in the northwestern US (July, August, September) together. The number of fires and the frequency of smoke in the atmospheric column peak between July and September in this region (Brey et al., 2018).

2.1.2. Surface Observations

We use in situ 24-hour average $PM_{2.5}$ observations from the EPA's Air Quality System (AQS) monitoring network (US EPA). The AQS network contains air pollution data collected by air quality monitors across the US maintained by the EPA, state, local, and tribal agencies. These data are collected from sites using both the gravimetric and beta-attenuation techniques and both 24-hr and 1-hr sample durations. We use $PM_{2.5}$ data from two sets of $PM_{2.5}$ monitors that exist in the AQS database: 1) federal reference method (FRM) and federal equivalent method (FEM) sites (EPA parameter code 88101) and 2) acceptable non-FRM sites that reasonably match the

FRM (EPA parameter code 88502). In order for the data from a given monitor to be included in our trend analysis at monitoring sites, data must be available for that monitor for every season between 2006 and 2016 and the monitor must have 80% data availability for the season each year. In total, trends in $PM_{2.5}$ are calculated for 413 unique $PM_{2.5}$ monitors across the US. At each monitoring site, we evaluate the trend in $PM_{2.5}$ using a linear least-squares regression (results in main text) as well as Theil-Sen estimator (results in Appendix 6.1). These two methods qualitatively agree, and the choice of method does not affect the conclusions of this work. The significance of the resulting best-fit lines is evaluated using a two-sided t-test with a null hypothesis that the slope is zero at a 95% confidence level.

2.1.3. Interpolation of Surface Observations

Surface monitors can be sparsely located in remote regions where wildfires often occur. To obtain a spatially continuous surface $PM_{2.5}$ estimate we interpolate between surface measurements using ordinary kriging. Kriging is an inverse-distance-weighted data interpolation method (Isaaks & Srivastava, 1990) that has been recently used in air quality research (e.g. Janssen et al., 2008; Lassman et al., 2017). Kriging estimates values between data points by assuming a functional form for the rate of decay of the sites spatial autocorrelation. We select a spherical semivariogram, which has been shown to work well in previous studies using kriging with air quality data (Lassman et al., 2017).

The function is fit using three parameters: nugget, sill, and range. The parameters are determined using a k-fold cross validation with ten folds. 2,700 different combinations of parameters are tested. Values tested for each parameter are as follows: sill: 0.2, 0.4, …, 2.8, 3.0; range: 0.5, 1.5,

…, 9.5, 10.0; nugget: 0.1, 0.2, …, 0.9, 1.0. The parameters are evaluated over the western US for May - October of 2015. For each set of parameters, the available monitoring sites were divided into ten unique groups (or 'folds') containing 101 monitors each (except the final group which contained 104 monitors). We remove one group of monitors and krige the remaining monitors to obtain a continuous estimate of $PM_{2.5}$ across the domain. We evaluate the kriged estimate against the $PM_{2.5}$ concentrations reported by the removed monitors for each day by calculating R^2, slope, mean bias, and mean absolute error. This process is repeated for each group of monitors. We then average the statistical parameters across the ten folds. The set of parameters used in this study was then selected from the 15 sets of parameters that produced an R^2 in the highest 10%, slope in the highest 10%, mean bias in the lowest 10% absolute values, and mean absolute error in the lowest 10%. Using this method we select the parameters: sill = 2.6, range = 8.5, nugget = 0.1.

We focus the kriging analysis on the summer season and include all surface sites with data available on a given day for each summer season between 2006 and 2016 in the interpolation. This allows us to retain the maximum number of possible sites for the interpolation on each day. Daily-average $PM_{2.5}$ values measured at these sites are kriged to a 15 x 15 km grid over the contiguous US. We calculate summer area-average $PM_{2.5}$ values over the US PNW and over the contiguous US using the gridded $PM_{2.5}$ estimates. The gridded estimates, rather than point measurements, are used to calculate the area-average summer $PM_{2.5}$ to reduce bias towards urban locations where a larger proportion of the monitors are concentrated.

2.1.4. Satellite Observations of Smoke Plumes

Smoke-specific $PM_{2.5}$ is estimated using in situ $PM_{2.5}$ observations concurrently with areal polygons of smoke extent from the Hazard Mapping System (HMS) (Brey et al., 2018; Rolph et al., 2009; Ruminski et al., 2006). A detailed description of the HMS fire location and smoke polygon dataset is given in Rolph et al. (2009). In brief, HMS is an interactive tool that relies on imagery from several satellites and trained satellite analysts to identify fire locations and smoke plumes across North America. The HMS smoke plume polygons are largely derived from visible satellite imagery from the GOES geostationary satellites. The smoke plume polygons indicate locations where there is likely smoke somewhere in the atmospheric column during daylight hours. The HMS smoke plume and fire detection dataset has been operational since 2005. We begin our study period in 2006 because this is the first full year where HMS smoke plumes are available. In general, the number and extent of HMS smoke plumes are conservative estimates of smoke occurrence in the atmospheric column (Brey et al., 2018).

2.1.5. Identifying Smoke-$PM_{2.5}$

To estimate the smoke contribution to local $PM_{2.5}$ concentrations, we first use HMS smoke plumes to flag potentially smoke-influenced days (referred to as smoke days). We then subset the data from each surface monitor into 1) days with no overlapping HMS smoke plume, and 2) days with an overlapping HMS smoke plume (smoke days). The first subset of data for a given monitor is used to estimate the seasonal-median $PM_{2.5}$ concentrations on non-smoke-influenced days. We acknowledge that there are limitations to this method identifying the magnitude of smoke-influence on $PM_{2.5}$. 1) Dilute smoke not identified by HMS may still influence $PM_{2.5}$ concentrations on days that do not overlap HMS plumes. 2) Smoke plumes identified by HMS

could be located above the surface and have little to no impact on surface $PM_{2.5}$. 3) HMS smoke plumes are identified from observations during daylight hours, while 24-hour $PM_{2.5}$ observations include overnight observations when smoke plumes can shift and go unnoticed by HMS. We will qualitatively address the potential severity of these limitations by comparing this method to the independent CTM method of determining smoke influence on $PM_{2.5}$.

We calculate the expected $PM_{2.5}$ concentration from non-smoke sources at each monitor as the seasonal median of days with no overlapping HMS smoke plume. We use the seasonal median value rather than the mean as it is less sensitive to the effect of smoke-influenced days with higher $PM_{2.5}$ concentrations that were missed by the HMS smoke plumes. We interpolate these non-smoke influenced seasonal $PM_{2.5}$ concentrations using ordinary kriging to obtain a continuous non-smoke influenced $PM_{2.5}$ estimate across the domain. A daily smoke $PM_{2.5}$ ($PM_{2.5}$ from biomass burning) concentration is then estimated as the difference between the daily-mean $PM_{2.5}$ concentration and the seasonal non-smoke influenced $PM_{2.5}$ concentration for locations included in HMS smoke polygons (we set smoke $PM_{2.5}$ concentrations to zero at locations outside of HMS smoke polygons). Smoke $PM_{2.5}$ concentrations are calculated at each interpolated grid cell on each day during the time period. We calculate the seasonal mean of the total $PM_{2.5}$ concentration, non-smoke $PM_{2.5}$ concentration, and smoke $PM_{2.5}$ concentration for each summer season over the 11-year period. We will refer to this method of estimating smoke $PM_{2.5}$ and trends as the monitor-HMS method.

2.1.6. Chemical Transport Model Simulations

We also use the GEOS-Chem CTM (geos-chem.org) version 11-01 to estimate the impact of wildfire smoke on US trends in $PM_{2.5}$. The model is driven by assimilated reanalysis meteorology from the Modern Era Retrospective Analysis for Research and Applications, Version 2 (MERRA2) produced by the NASA Global Modeling Assimilation Office (Gelaro et al., 2017). Globally, we use the Emissions Database for Global Atmospheric Research (EDGAR) v4.2 anthropogenic emissions inventory with regional overwrites (Olivier et al., 1995). In the US, we follow the convention in GEOS-Chem version 12-01 where the EDGAR emissions are overwritten by the EPA NEI 2011 scaled for each year from 2006-2016 (Travis et al., 2016). Biogenic emissions are provided by the Model for Emissions of Gasses and Aerosols from Nature (MEGAN) (Guenther et al., 2012). We use biomass burning emissions of aerosol and gas-phase species from Global Fire Emissions Database version 4 (GFED4) at a 0.25^{o}x0.25^{o} resolution (Giglio et al., 2013; van der Werf et al., 2010).

We run global GEOS-Chem simulations from 2006-2016 with 1-month spin up at 2°x2.5° resolution with 47 vertical layers between the surface and 0.01 hPa. The model includes tracers for hydrophobic and hydrophilic black carbon (BCPO, BCPI), hydrophobic and hydrophilic organic carbon (OCPO, OCPI), dust (DST), sea-salt aerosol (SALA), inorganic sulfur nitrates (NIT), ammonium (NH4), and sulfate (SO4). Monthly mean $PM_{2.5}$ concentrations were calculated according to,

$$PM_{2.5} = 1.33\,(NH4 + NIT + SO4) + BCPI + BCPO + 2.1\,(OCPO + 1.16\,OCPI) + DST1 + 0.38\,DST2 + 1.86\,SALA, \quad (1)$$

where DST1 and DST2 are dust aerosol with an effective radius of 0.7 μm and 1.4 μm, respectively. To determine the impact of fires on $PM_{2.5}$, we use a pair of simulations. One simulation includes all emissions and the second simulation includes all emissions except the biomass burning emissions from GFED4. With this pair of simulations, we can isolate the impact of biomass burning on trends in simulated $PM_{2.5}$. Smoke $PM_{2.5}$ was identified as the difference between monthly $PM_{2.5}$ with biomass burning on and off.

2.2. Results and Discussion

2.2.1. Seasonal Trends in $PM_{2.5}$ Observed at Surface Sites

Observed trends in seasonal-mean $PM_{2.5}$ at contiguous US sites are shown in Figure 1 for the period 2006 to 2016. In line with previous several studies (Blanchard et al., 2013; Hand et al., 2011; Murphy et al., 2011; Schichtel et al., 2001), we find a predominantly negative trend in seasonal-mean $PM_{2.5}$ in all seasons. The largest reductions in absolute $PM_{2.5}$ concentrations occurred in spring and summer in the eastern US during this time period. In these regions over our 11-year study period, the rate of decline in $PM_{2.5}$ was as large as -1.67 μg m^{-3} yr^{-1}, which occurred in Liberty, Pennsylvania in the summer season. Significant declines in $PM_{2.5}$ are ubiquitous across the eastern US in all seasons: the $PM_{2.5}$ trends are significantly negative at 45%, 59%, 44%, and 55% of sites east of 100^{o} W in winter, spring, summer, and fall, respectively.

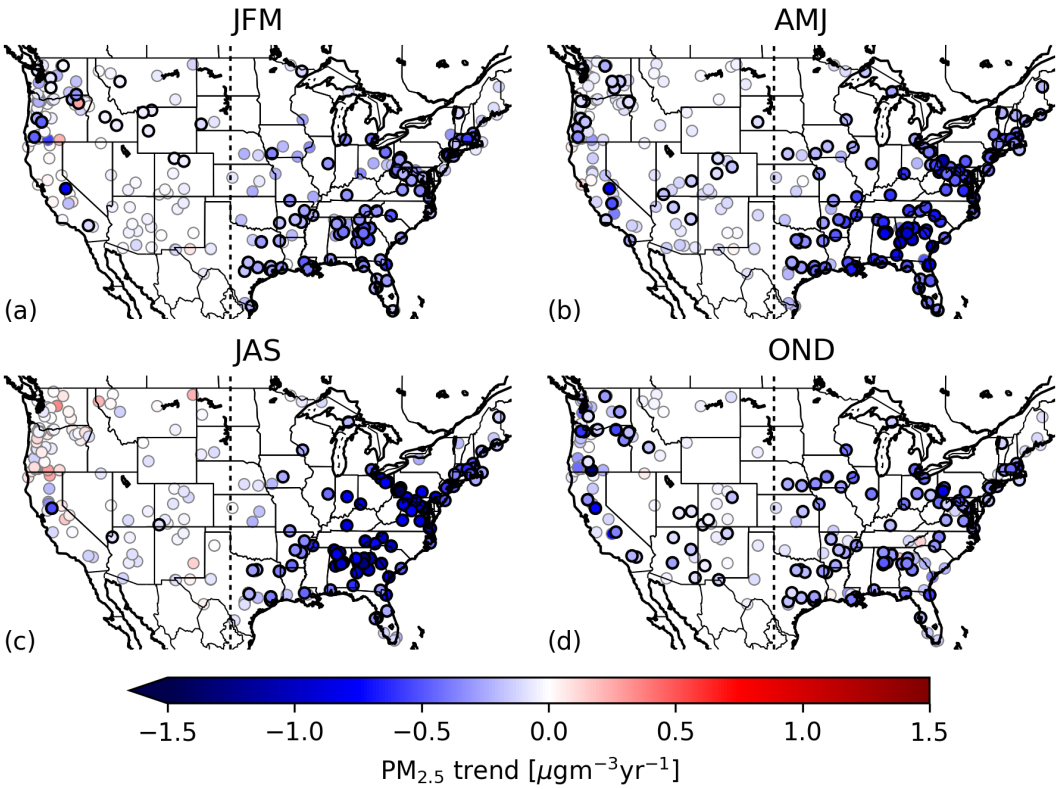

Figure 1. Slopes of linear fits on seasonal-mean $PM_{2.5}$ at EPA AQS sites from 2006-2016. Sites with slopes that are significantly different from 0 at the 95% confidence level are outlined in black, and sites with insignificant slopes are outlined in gray. Dashed line drawn at 100° W is used in the analysis to distinguish between the eastern and western US.

In contrast to the eastern US, fewer sites in the western US exhibit significant declines in total $PM_{2.5}$. The percent of sites in the western US (west of 100° W) that exhibit a significant decrease in $PM_{2.5}$ is 20%, 26%, and 37% over winter, spring, and fall. In summer (Figure 1c), only 4 sites (less than 5 % of sites studied in the western US) exhibit a significant decline in $PM_{2.5}$ over this period; 42 of the 73 sites studied in the PNW (represented by the gray box in Figure 2) report positive but insignificant trends in summer-mean $PM_{2.5}$ over the time period. This is in agreement with prior work on summer $PM_{2.5}$ trends observed at surface monitors over previous years (Hand et al., 2011; Murphy et al., 2011). We investigate whether these positive trends in total $PM_{2.5}$ can be attributed to positive trends in smoke $PM_{2.5}$.

2.2.2. Trends in Smoke and Non-Smoke $PM_{2.5}$

Figure 2 presents trends in total, non-smoke, and smoke- influenced $PM_{2.5}$ using the monitor-HMS method (panels a, b, c) with 15 km resolution and GEOS-Chem with 2 x 2.5° resolution

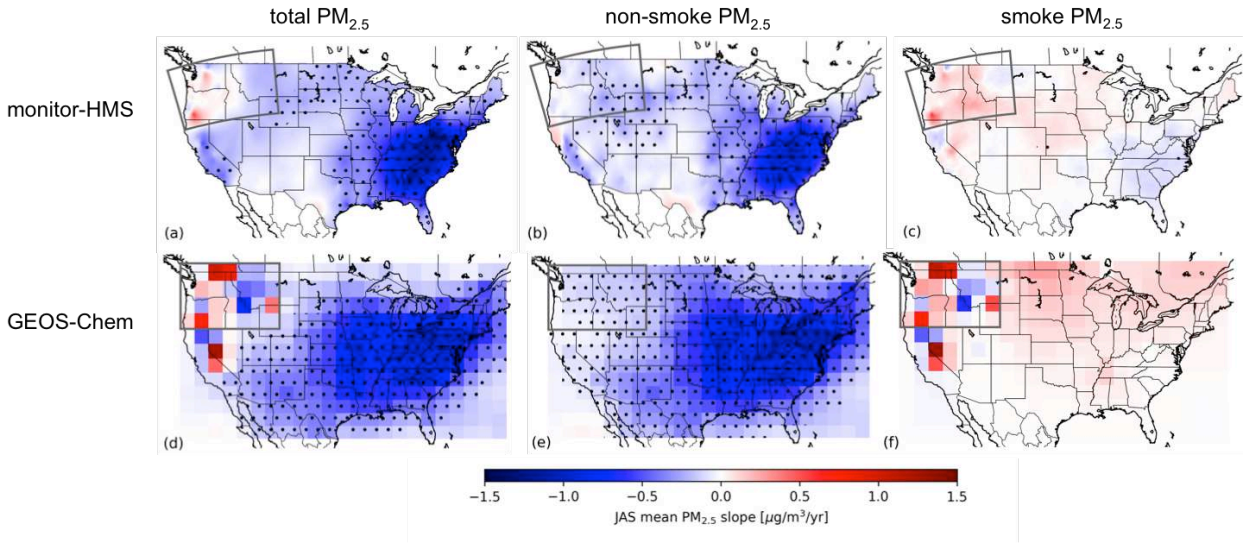

Figure 2. Slopes of linear fits on summer-mean (JAS) total $PM_{2.5}$, non-smoke $PM_{2.5}$, and smoke $PM_{2.5}$ from 2006-2016 for the monitor-HMS (panels a, b, and c) and the GEOS-Chem model (panels d, e, and f) methods. Locations with slopes significantly different from zero at the 95% confidence level are dotted. Gray boxes define the Pacific Northwest region.

(panels d, e, and f). By including CTM estimates in our analysis, we are able to identify discrepancies between observed and simulated trends in $PM_{2.5}$ over the past decade. In general, the model and monitor-HMS approaches agree in the location and sign of trends in summer-mean total $PM_{2.5}$. GEOS-Chem predicts a larger spatial extent in significant negative trends in $PM_{2.5}$ compared to the monitor-HMS method. In the PNW and northern California, the two approaches disagree about the location, sign, and magnitude of the trends in total $PM_{2.5}$. The inconsistent patterns in $PM_{2.5}$ trends in the PNW and northern California shown in both estimation methods are reflected in the observations from monitoring sites in the region (see Figure 1c). There are $PM_{2.5}$ data records that have both increased and decreased at different

monitoring sites in the PNW and northern California over this time period likely due to high interannual variability in wildfire smoke concentration.

Trends in non-smoke $PM_{2.5}$ are shown in Figures 2b and 2e. In the absence of smoke influence, the spatial extent of significant negative changes in $PM_{2.5}$ expands for both the model and the monitor-HMS method. The monitor-HMS method shows significant declines in $PM_{2.5}$ across Idaho, Colorado, and Utah while GEOS-Chem shows significant declines in $PM_{2.5}$ across most of the country. Both GEOS-Chem and the monitor-HMS method produce small negative, or insignificant, changes in non-smoke $PM_{2.5}$ across most of the PNW. Despite several differences between the two methods of attributing smoke $PM_{2.5}$, both estimation methods suggest that decreases in summer-mean $PM_{2.5}$ would be expected over more of the West in the absence of wildfire smoke.

Figures 2c and 2f show linear trends in smoke $PM_{2.5}$. Both the monitor-HMS-based and GEOS-Chem-based estimates produce an insignificant increase in smoke $PM_{2.5}$ in Oregon and Washington over this period and an insignificant decrease over portions of Montana. Both methods show small positive smoke $PM_{2.5}$ trends over the northern Great Plains and New England, but the two methods disagree on the sign of the changes in the Southeast. Simulated surface $PM_{2.5}$ concentrations in GEOS-Chem are likely more sensitive to changes in fire emissions than reality because all biomass burning emissions in the version of the model we used here are emitted at the surface. However, on average, a large fraction of the smoke from fires in the PNW and Canada are emitted above the boundary layer (Zhu et al., 2018). A possible origin for the disagreement between the monitor-HMS-based and GEOS-Chem-based estimates in the

Southeast is our inability to completely isolate smoke $PM_{2.5}$ from total $PM_{2.5}$ in the observations due to the limitations of satellite-smoke plume estimates discussed in the methods.

2.2.3. Wildfire Smoke Contributions to Summer-Mean $PM_{2.5}$ in the PNW

In Figure 3, we focus on area-averaged summer-mean $PM_{2.5}$ in the PNW (the grey boxes outlined in Figure 2), where Figure 2 demonstrated most of the increases in summer-mean $PM_{2.5}$.

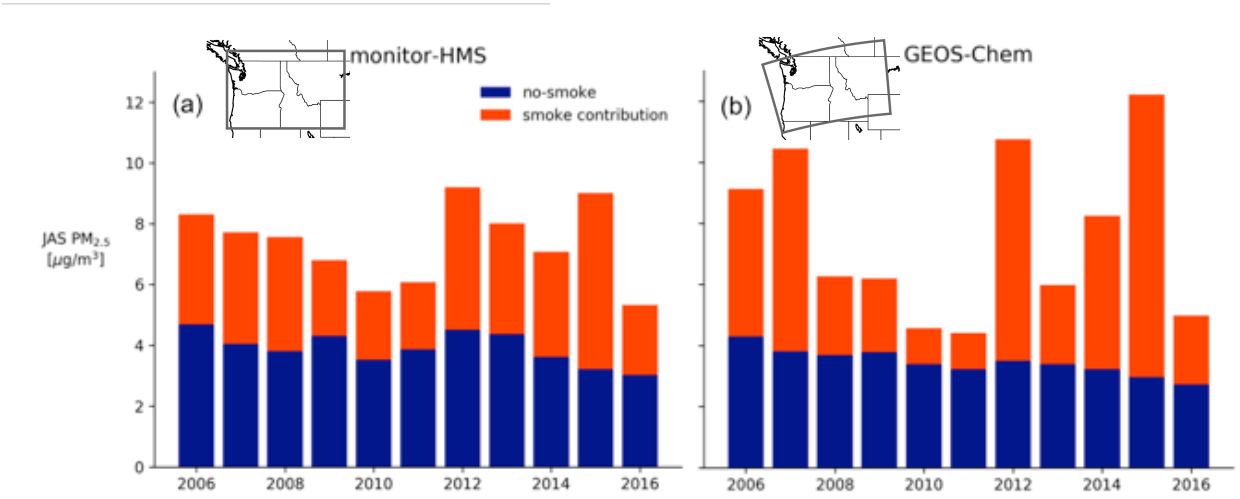

Figure 3: Estimated smoke contribution to area-averaged summer (JAS) mean $PM_{2.5}$ across the Pacific Northwest, defined by the gray box in Figure 2, using the monitor-HMS method (panel a) and GEOS-Chem (panel b). The full height of each bar represents the summer mean of total $PM_{2.5}$. Estimated summer-mean $PM_{2.5}$ on days without smoke influence is shown in blue, and the difference (the estimated smoke contribution) is shown in orange.

We separate the summer-mean $PM_{2.5}$ for this region into a non-smoke mean $PM_{2.5}$ concentration (what we would expect the summer-mean $PM_{2.5}$ to be in the absence of wildfire smoke), and the mean smoke contribution to the summer-mean $PM_{2.5}$. The smoke contribution, shown in orange, is the difference between the total summer-mean $PM_{2.5}$ (total height of each bar) and the estimated non-smoke mean $PM_{2.5}$ (blue section of each bar). During the 11-year study period, wildfire smoke contributes between 2.2 and 5.8 $\mu g\ m^{-3}$ (monitor-HMS, Figure 3a) or 1.2 and 9.2 $\mu g\ m^{-3}$ (GEOS-Chem, Figure 3b) of the summer-mean $PM_{2.5}$ in the PNW, depending on the year.

For several summers during active fire seasons, wildfire smoke contributes over 50% of the summer-mean $PM_{2.5}$ according to both methods. The year with the largest contribution in this region according to both methods is 2015 with smoke contributing 64% of the summer-mean $PM_{2.5}$ using the monitor-HMS-based approach and 76% using the GEOS-Chem-based approach. There were many large fires in this region during 2015, and smoke impacted wide swaths of the US (e.g. Ford et al., 2017; Lindaas et al., 2017; Wettstein et al., 2018). Despite the fact that wildfires are typically sporadic and transient events, both methods indicate that wildfire smoke can greatly increase the summer-mean $PM_{2.5}$, especially in years with many large fires.

In the absence of wildfire smoke, there is much less inter-annual variability in summer-mean $PM_{2.5}$ (Figure 3). Both of our approaches indicate that without the influence of smoke, we would expect modest improvements in summer-mean $PM_{2.5}$ in the PNW in line with improvements elsewhere in the US. Both approaches produce a ~ 1% decrease in summer-mean $PM_{2.5}$ per year across this region in the absence of smoke $PM_{2.5}$. A linear fit on the non-smoke mean $PM_{2.5}$ from the GEOS-Chem approach yields a slope of -0.12 $\mu g\ m^{-3}\ yr^{-1}$ ($R^2 = 0.85$, p-value = 5.15×10^{-5}); a linear fit on the monitor-HMS estimates yields a similar slope of -0.10 $\mu g\ m^{-3}\ yr^{-1}$ ($R^2 = 0.39$, p-value = 0.04). We do not find statistically significant increases in the area-average summer-mean $PM_{2.5}$ attributed to smoke over the 11-year study period using either the monitor-HMS (slope = 0.05 $\mu g\ m^{-3}\ yr^{-1}$, $R^2 = 0.02$, p-value = 0.65) or GEOS-Chem approaches (slope = 0.10 $\mu g\ m^{-3}\ yr^{-1}$, $R^2 = 0.02$, p-value = 0.71). We note that linear trendlines are highly dependent on the start and end years of the fit (here ending on an exceptionally low fire year), and there was a large interannual variability in the contribution of smoke to $PM_{2.5}$ during this period (e.g. Figure 3).

In Figure 4, we investigate two factors that are likely drivers of summer smoke $PM_{2.5}$ trends, (1) the frequency of smoke days and (2) $PM_{2.5}$ concentrations on smoke days. The first case corresponds to the average fraction of the PNW with smoke in the column (from HMS) in each

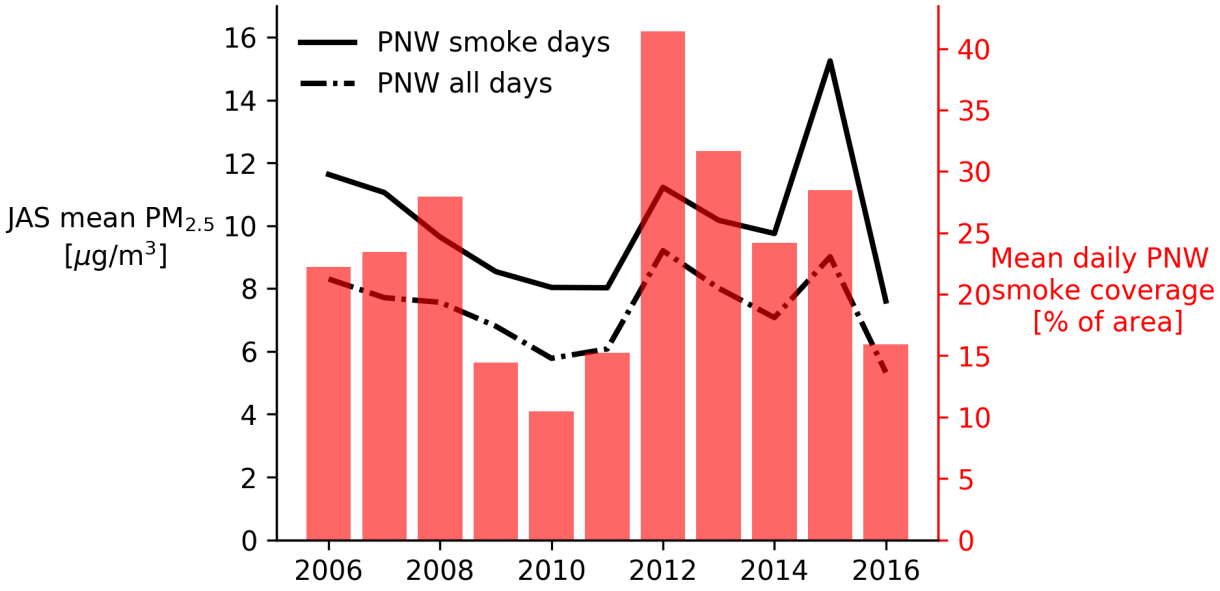

Figure 4: *Left axis*: Dot-dashed line shows the area-averaged summer (JAS) mean $PM_{2.5}$ estimated using the monitor-HMS method on all days across the Pacific Northwest (PNW). Solid line shows the summer-mean $PM_{2.5}$ on potentially smoke-influenced days in the PNW. *Right axis*: the red bars represent the average fraction of PNW area covered by a smoke plume during the summer.

summer. The second case is the $PM_{2.5}$ concentrations in areas with smoke in the column. Hence, we are investigating if variability in smoke $PM_{2.5}$ in the PNW is due to variability in smoke area or smoke concentrations. The mean fraction of total area in the PNW with smoke somewhere in the column on a given summer day ranges from 10 - 15% in low fire years (e.g. 2010) to >40% in extreme years (e.g. 2012). The summer-mean $PM_{2.5}$ concentrations on smoke days range from 7.6 μg m^{-3} in low fire years to 15 μg m^{-3} in high fire years according to the monitor-HMS method. There is a weak correlation between the two cases (R^2 = 0.36); big fire years tend to have higher values for both metrics. However, some high-smoke years are more driven by

extensive smoke spatial coverage (e.g. 2012) while others are more driven by higher smoke-day $PM_{2.5}$ concentrations (e.g. 2015). Large interannual variability in both the area covered by smoke and $PM_{2.5}$ on smoke days obscures decreasing trends in non-smoke summer-mean $PM_{2.5}$ in this region (Figures 3 and 4).

3. THE USE OF SOCIAL MEDIA TO IMPROVE MODELS OF WILDFIRE SMOKE EXPOSURE

3.1. Methods

3.1.1. Time Period and Domain

We focus our analysis on the western US, defined by the gray shaded region in Figure 5. We study the 2015 wildfire season, when portions of the western US were impacted by many large fires and elevated smoke concentrations, as shown in chapter 2. The study period, 5 June – 30 September 2015, is defined by the western US wildfire season (typically June – September) and data-availability. The Facebook posts are available 5 June – 27 October 2015.

3.1.2. Chemical Transport Model Simulations

We use the Weather Research and Forecasting model with Chemistry (WRF-Chem) to simulate surface $PM_{2.5}$ concentrations. WRF-Chem is a CTM that couples atmospheric dynamics and chemistry (Grell et al., 2005). CTMs are a useful tool to estimate exposure as they provide information on $PM_{2.5}$ concentrations between surface monitoring sites. However, they are computationally expensive and may be incorrect due to errors in meteorology, fire locations, emission rates, and injection heights.

For this work we use the WRF-Chem model version 8.3.1. The model domain is represented by the gray shaded region in Figure 5. We use Global Forecast System (GFS) initial and boundary conditions, Yonsei University boundary-layer parameterization (Hu et al., 2010), and the

Thompson microphysics parameterization (Thompson et al., 2004). We reinitialize the meteorology each day to minimize drifting from meteorology observations. For the chemistry initial/boundary conditions and mechanisms we use the Model for Ozone and Related chemical Tracers (MOZART) (Emmons et al., 2010) with the Goddard Chemistry Aerosol Radiation and Transport (GOCART) model (Chin et al., 2000).

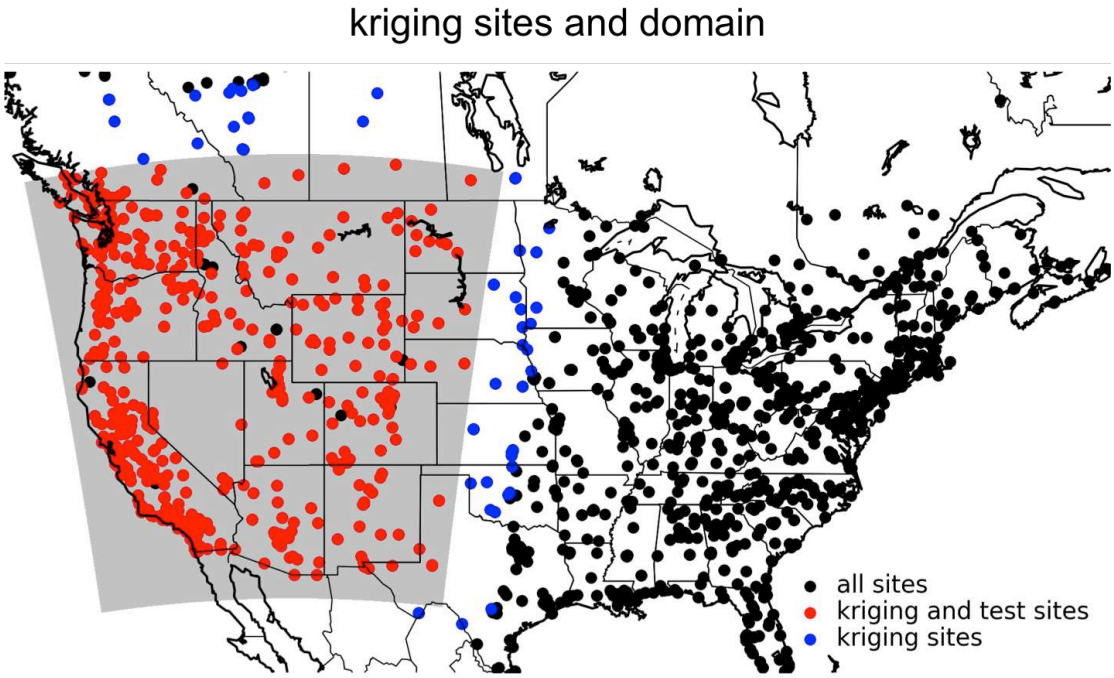

Figure 5: The WRF-Chem/kriging domain is represented by the gray shading. Surface sites from the EPA AQS network used in this study are represented by the colored dots. Red dots represent sites used in the kriging estimates and to evaluate the kriging. Blue dots represent sites used in the kriging estimates, but not used in the evaluation because they are outside of the domain. All remaining sites are shown in black. Note: black dots within the kriging domain represent sites with no available data during the study period.

We use anthropogenic emissions from the EPA NEI 2011 emissions inventory (US EPA), biogenic emissions from the Model for Emissions of Gasses and Aerosols from Nature (MEGAN) (Guenther et al., 2012), and biomass burning emissions from the Fire Inventory from NCAR (FINN) (Wiedinmyer et al., 2011). Injection heights of pollutants in WRF-Chem are determined using a 1-D plume rise parameterization (Freitas et al., 2007). Using this model set-

up, we simulate daily-average surface $PM_{2.5}$ concentrations at 15 km x 15 km resolution over the western US for each day during the study period.

3.1.3. Interpolated Surface Observations

In this study, we use an interpolation approach similar to that described in Section 2.1.3. We use ordinary kriging with the same semivariogram model and parameters. In this study, we do not remove sites based on seasonal data-availability as was done with the trends analysis. For each day in the study period, we krige all available daily $PM_{2.5}$ observations from both FRM sites and sites that reasonably agree with the FRM in the EPA AQS network. (See section 2.1.2 for further detail on the EPA AQS surface sites.) We krige the daily observations to the WRF-Chem grid, shown along with the kriging sites in Figure 5.

3.1.4. Satellite Observations

We use aerosol optical depth (AOD) from the Moderate Resolution Imaging Spectroradiometer (MODIS) instrument. AOD is a measure of the optical path extinction by particles in a vertical column (here the full atmospheric column), and is often used as a proxy for $PM_{2.5}$ (Li et al., 2015). Although AOD is a column measurement, it can be well correlated with surface measurements of $PM_{2.5}$ is some regions of the US (e.g. Engel-Cox et al., 2004; Ford & Heald, 2013; Li et al., 2015). AOD can be related to surface $PM_{2.5}$ with an estimated scaling factor (e.g. van Donkelaar et al., 2010). Here, the conversion of AOD to $PM_{2.5}$ is determined by the weighted regression coefficients calculated by the blended model described in section 3.1.6.

The MODIS instrument is located onboard the Aqua and Terra satellites with local overpass times of 1:30 P.M. and 10:30 A.M., respectively. The MODIS instrument uses 36 different electromagnetic wavelengths to observe the Earth's surface. We use the Level 2 AOD Dark-Target Collection 6 retrieval with 10 km spatial resolution (Sayer et al., 2014). The twice-daily retrievals of AOD at a 10 km resolution are re-gridded to the 15 x 15 km WRF-Chem grid by taking the average of all MODIS grid cells that fall within the larger WRF-Chem grid cell. We then average the two daily AOD retrievals from the Aqua and Terra overpasses for each grid cell to obtain a daily average MODIS AOD estimate on the WRF-Chem grid.

The AOD-retrievals often have missing pixels due to a cloud-masking algorithm in the data processing code. Dense smoke plumes are frequently miss-classified as clouds by this algorithm and are subsequently removed from the final data product (van Donkelaar et al., 2011). To retain AOD estimates of smoke plumes, we fill in missing pixels in the Aqua and Terra composite AOD by the same method used in Lassman et al. (2017). Any grid cell that has at least 3 surrounding data points is assigned the average of the surrounding AOD values. This processes is repeated five times. We stop filling in pixels after five iterations because after this point less than 5% of the remaining missing values are filled in by each subsequent iteration. By filling in these missing pixels, we are able to increase the data-completeness of the AOD retrievals from 61% to 85% across the full study period and domain. An example day of filling in mixing pixels is shown in Figure 6.

Satellite observations are beneficial for exposure classification because they can provide a continuous gridded product at sub-daily frequency. This is an advantage over sparsely located

surface observations, many of which only provide observations every three days. However, using satellite-derived AOD to assess surface $PM_{2.5}$ concentrations comes with several disadvantages. 1) The accuracy of AOD retrieval is highly dependent on surface properties, 2) the AOD:surface-$PM_{2.5}$ ratio varies with smoke plume height, aerosol properties, and the presence of clouds, 3) smoke plumes can often be misinterpreted as clouds in the retrieval algorithm and removed from the final AOD product.

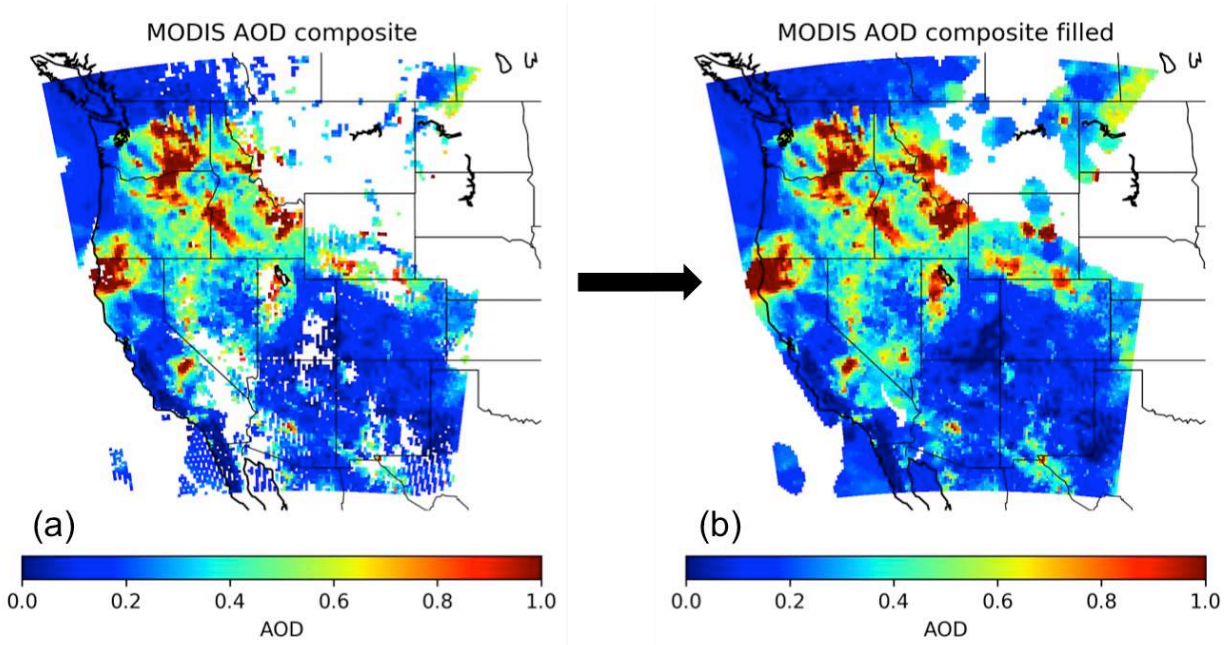

Figure 6: An example day (August 18, 2015) of the MODIS AOD pixels filled in using the filling algorithm, described in the methods, to fill in pixels of dense smoke often misclassified as clouds and removed from the data. Data before filling in missing pixels is shown in panel a and the data post-filling in mixing pixels is shown in panel b.

3.1.5. Social Media

In this study, we use the same dataset of Facebook posts described in Ford et al. (2017). The dataset is composed of de-identified, aggregated percent of Facebook posters in a town or city with posts containing keywords related to smoke exposure, while controlling for posts related to cigarette-smoke and those not related to air quality. These words include: "smoke", "smoky", "air quality", "hazey", etc. The Facebook posts are population-weighted and gridded to the

WRF-Chem grid shown in Figure 5. A full list of search terms and filtered phrases as well as a detailed description of the Facebook dataset is given in Ford et al. (2017). Ford et al. (2017) find that the performance of Facebook posts in predicting surface $PM_{2.5}$ concentrations is dependent on cloud fraction (CF). Posters appear be less likely to post about being in smoke when it is cloudy. In their study, Ford et al. (2017) distinguishes Facebook posts on high CF days (CF > 75%) and low CF days (CF < 75%). We take a similar approach in this study. We use CF products ("cloud_fraction_land" and "cloud_fraction_ocean") from the MODIS instrument on the Terra and Aqua satellites. The CF retrievals from the twice-daily overpasses are combined and re-gridded using the same process described in section 3.2.3 used to process the AOD retrievals.

3.1.6. Blending Datasets Using Geographically Weighted Ridge Regression

We calculate a blend of the three datasets using a geographically weighted ridge regression (GWR), a method recently applied to air-quality studies (van Donkelaar et al., 2015; Lassman et al., 2017; Luo et al., 2017; Song et al., 2014). We follow a similar data blending approach to that described in Lassman et al. (2017). In brief, we calculate a set of linear ridge-regression coefficients at each surface monitor location by removing that monitor's $PM_{2.5}$ measurement from the dataset then estimating $PM_{2.5}$ at the monitor location using kriging, WRF-Chem, MODIS AOD, and Facebook posts. A unique set of regression coefficients is calculated for each surface monitor location within the domain. The regression coefficients weight each dataset in the blend allowing for a blended estimate using the following equation,

$$PM2.5_{GWR} = A + B\times AOD + C\times PM2.5_{kriging} + D\times PM2.5_{GEOS\text{-}Chem} + E\times(\text{percent of Facebook posts}) \quad (2)$$

where A is the fitted intercept parameter, and B, C, D, and E are the fitted regression coefficients. In this equation B and E also account for the $PM_{2.5}$:AOD ratio and $PM_{2.5}$: percent of Facebook posts at each monitoring site, respectively. By calculating separate regression coefficients at each monitor site, this regression method allows the datasets to be weighted differently in locations where their utility may differ within the domain (e.g. urban versus rural areas). The regression coefficients at the surface-monitor locations are interpolated throughout the domain using a Gaussian kernel,

$$G = \exp(-(D/B_w)^2), \quad (3)$$

where G is the kernel value for each surface monitor, D is the distance to a grid cell from the surface monitor, and B_w is the bandwidth parameter which we define as 500 km. Interpolating the regression coefficients allows us to estimate $PM_{2.5}$ concentrations between surface monitor sites at each grid cell within the domain. Figure 7 shows a sample blend of the kriging, WRF-Chem simulations, MODIS AOD, and percent of Facebook posts using GWR for an active fire day in the western US during 2015.

We calculate four sets of GWR blends to use throughout the domain. The sets of blends using different subsets of the input datasets are listed in Table 1. We use the four sets of blends to account for discontinuous datasets (e.g. missing AOD pixels) and to account for the impact of

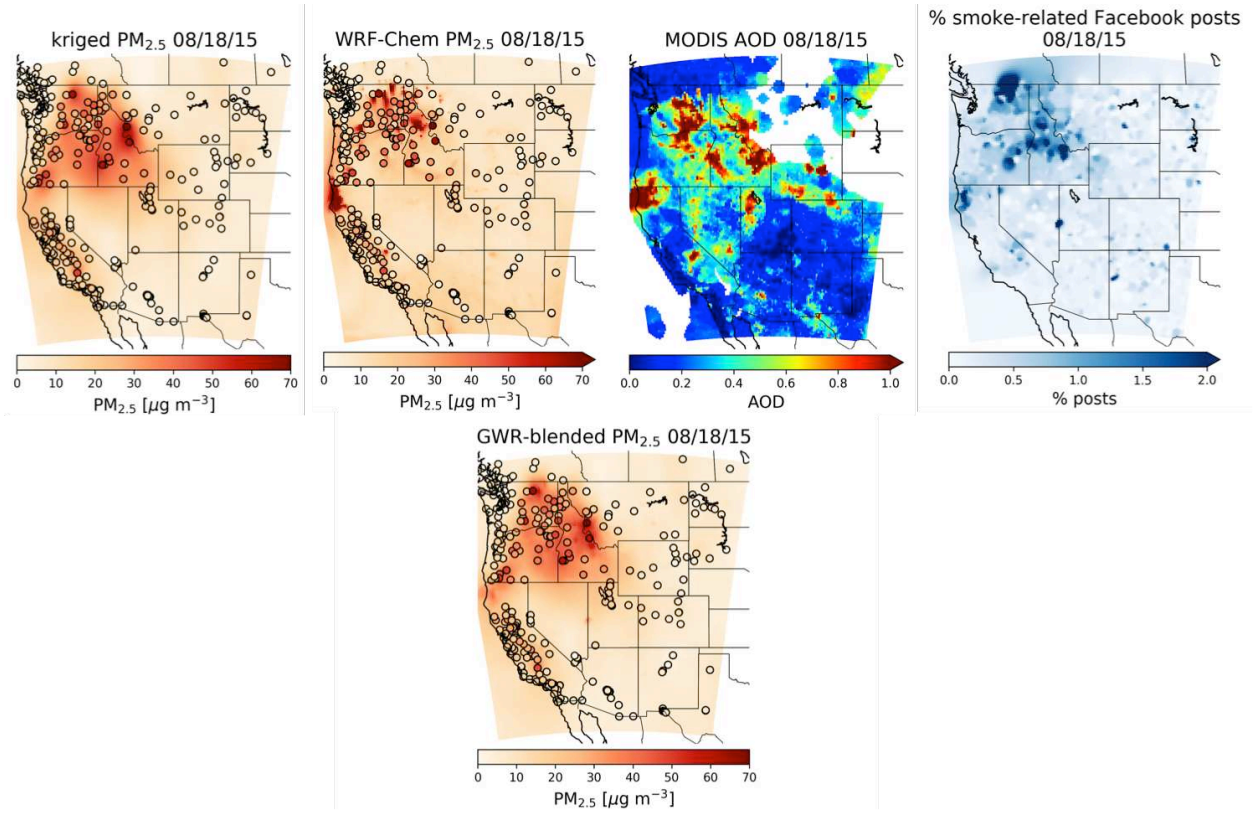

Figure 7 - Sample day (August 18, 2015) of each individual dataset regrided to the WRF-Chem grid: a) kriged surface monitors, b) WRF-Chem simulated $PM_{2.5}$, c) MODIS AOD, and d) population-weighted Facebook posters. The GWR blended estimate of the datasets shown in panels a-d, is shown in panel e. In panels a, c, and e surface monitor-observed 24-hr average $PM_{2.5}$ are also shown. Note: the GWR blended $PM_{2.5}$ presented here does not take CF into account for the Facebook dataset.

Table 1*:* List of separate GWR blends and input variables used to account for MODIS AOD-availability at individual grid cells and the impacts of CF on the Facebook data.

Days/grid cells where GWR estimate is used	**Input variables**	**Days used to calculate GWR regression coefficients at surface sites**
High CF with available AOD	Kriged surface monitors, MODIS AOD, WRF-Chem, Facebook data	High CF days for each surface site
Low CF with AOD available	Kriged surface monitors, MODIS AOD, WRF-Chem, Facebook data	Low CF days for each surface site
High CF, without AOD	Kriged surface monitors, WRF-Chem, Facebook data	High CF days for each surface site
Low CF, without AOD	Kriged surface monitors, WRF-Chem, Facebook data	Low CF days for each surface site

CF on the accuracy of the Facebook dataset in predicting surface $PM_{2.5}$ concentrations. The high/low CF GWR blends are calculated as follows: We divide the input datasets into two groups based on CF. The high CF group contains all days and surface sites where the CF is greater than 0.75, and the low CF group contains all data points where the CF is less than 0.75. We use these two subsets of data points to calculate GWR regression coefficients at each surface site across the domain. The regression coefficients are then interpolated throughout the domain, described previously. The value of 0.75 was chosen because this was the high/low CF cutoff used by Ford et al. (2017).

We combine the subsets of blends into a final GWR blended estimate by using the blend from the subset of blended datasets that is most appropriate for each individual grid cell on each day of the study period. For example, if a grid cell has a high cloud fraction and no AOD estimate for that day, we use the high CF GWR blend of kriging, WRF-Chem, and Facebook blended $PM_{2.5}$ estimate for that grid cell. This process is repeated for each grid cell on each day of the study period. This process ultimately produces two final GWR blended datasets, one including the Facebook dataset as an input variable, and one without.

3.1.7. Evaluation of Datasets

We evaluate each individual dataset and the blended datasets against $PM_{2.5}$ concentrations reported by surface monitors in the EPA AQS monitor network. For the MODIS, WRF-Chem, and Facebook posts gridded datasets, each grid cell containing a surface monitor is evaluated against that surface monitor's measured $PM_{2.5}$ values. The kriged surface monitor dataset and GWR-blended data (which uses the kriged surface monitor dataset) are evaluated using the

"leave-one-out cross-validation" technique (Efron, 1982) to overcome the potential bias of evaluating these estimates using the same surface monitors that were used to create the interpolated and blended data sets. This technique acts to mitigate the aforementioned bias by removing a surface monitor from the interpolation, re-calculating the interpolated concentration/regression coefficients, and comparing the interpolated concentration/$PM_{2.5}$ estimated using the regression equation at the location of the removed monitor to the value measured by the monitor. This process is repeated for all sites in the domain.

3.2. Results and Discussion

3.2.1. Performance of Individual Datasets

The performance of each individual dataset against the surface monitors is shown in Figure 8.

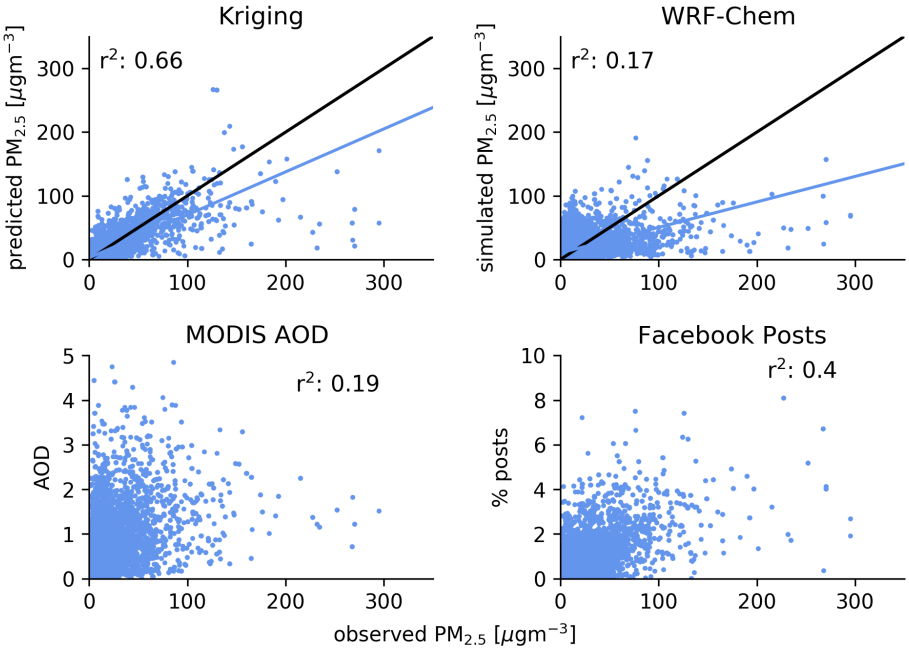

Figure 8: Performance of each individual dataset against surface-monitor observed $PM_{2.5}$: a) kriging, b) WRF-Chem, c) MODIS AOD, d) Facebook posters. Each day and site during the study period is represented by the blue dots. Blue lines represent linear-least squares best-fit lines. Black lines in panels a and b show a 1-1 line. These lines are not shown in panels c and d because these datasets do not explicitly estimate $PM_{2.5}$; a 1-1 fit is not expected.

Similar to the results from Lassman et al. (2017), the kriged surface monitor dataset best predicts surface monitor concentrations overall with an R^2 = 0.66. In agreement with the results from Ford et al. (2017), the Facebook dataset outperforms both WRF-Chem and MODIS AOD with an R^2 = 0.4 compared to 0.17 and 0.19, respectively. Figure 9 shows how the overall performance of each dataset is distributed among the surface sites.

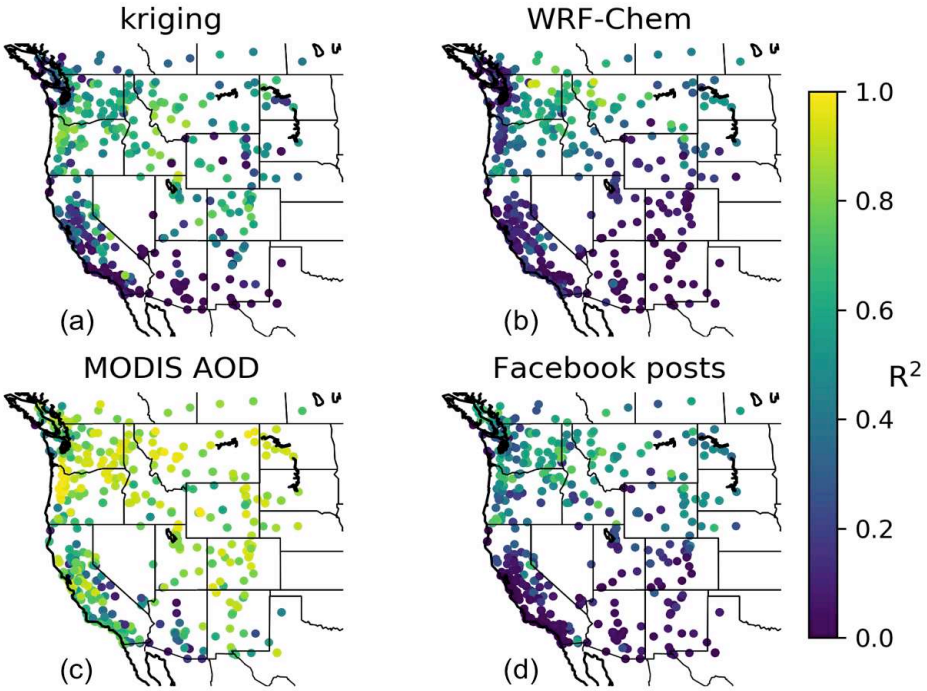

Figure 9: R^2 between each dataset and observed surface-monitor $PM_{2.5}$ at each monitor within the domain: a) kriging, b) WRF-Chem, c) MODIS AOD, d) Facebook posters. Only sites with at least 30 observations during the time period are shown.

In general, each dataset has higher R^2 values at surface sites in the northern part of the domain than the southern. This is likely due to the larger fluctuations in $PM_{2.5}$ in that region from a larger influence of wildfire smoke. The datasets have a greater ability to capture these large fluctuations in $PM_{2.5}$ in this region, compared to the predominately smaller fluctuations in the southwest, increasing the R^2.

3.2.2. Performance of Blended Dataset with and without Facebook

In Figure 10, we present the performance of the blended dataset both with and without Facebook data evaluated against surface-monitor observed $PM_{2.5}$. According to each of the performance-

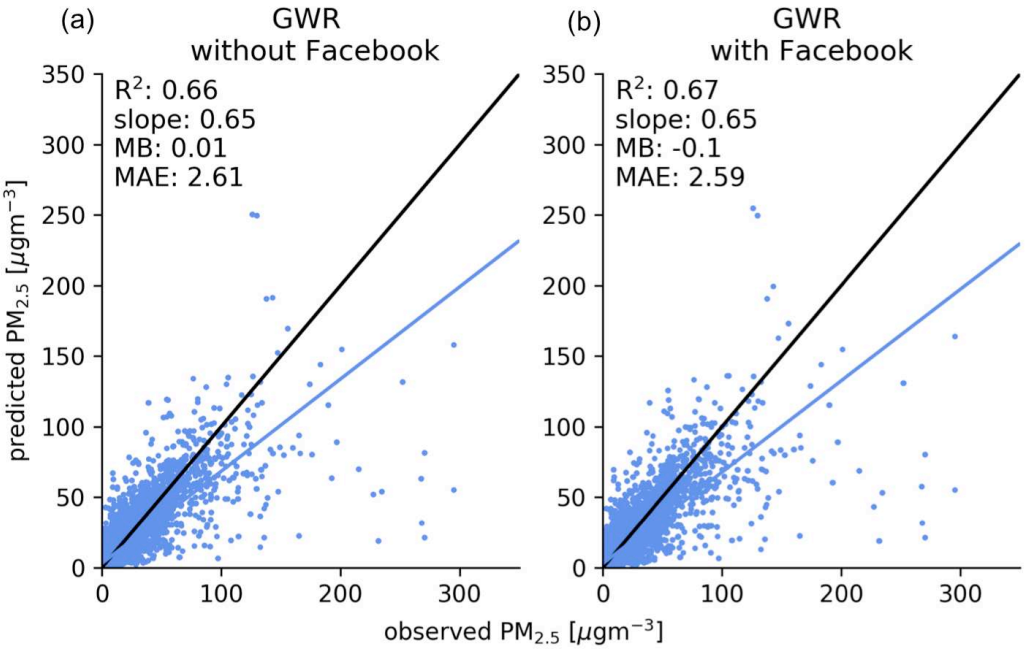

Figure 10: Performance of the GWR blended data against surface-monitor observed $PM_{2.5}$ without (panel a) and with (panel b) Facebook posts as an input variable. Performance-assessing metrics: R^2, slope, mean bias (MB), and mean absolute error (MAE) are shown. Each day and site during the study period is represented by blue dots. Blue lines represent linear-least squares best-fit lines and black lines represent a 1-1 line.

assessing metrics we use, the addition of Facebook posts to the blended data makes little or no difference in the overall performance of the dataset. In Figure 11 we show the change in R^2 at the individual sites within the domain. Overall, there is little or no change at most monitoring sites (note the small scales on the absolute change color bar). Although not shown in Figure 11, there is also little change at most surface sites in all other performance-assessment metrics used. These

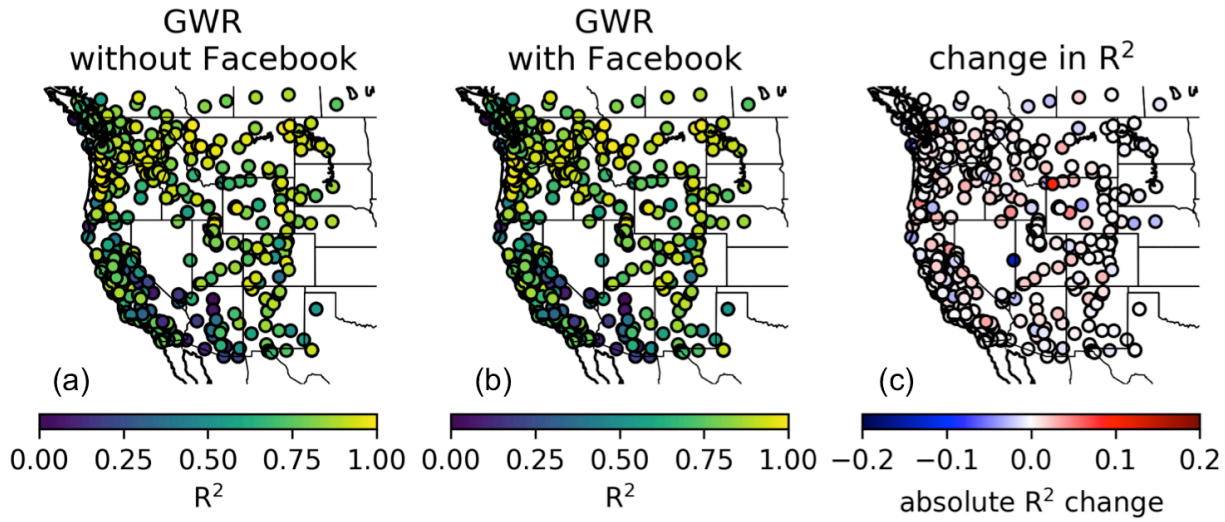

Figure 11 - The change in R^2 at each individual monitoring site with the addition of Facebook to the GWR blend. R^2 between surface-monitor observed $PM_{2.5}$ and the GWR blend without Facebook is shown in panel a. R^2 between surface-monitor observed $PM_{2.5}$ and the GWR blend with Facebook is shown in panel b. The absolute change in R^2 between panels a and b is shown in panel c. Note the relatively small color bar scale in panel c.

include: slope, mean bias, and mean absolute error. The cause for the lack of influence of the Facebook data is revealed in Figures 12 and 13.

In Figure 12 we show the weight given to each dataset at the individual monitoring sites. Weights of the Facebook and MODIS datasets, which do not directly provide surface $PM_{2.5}$ concentrations, are normalized by the mean Facebook:$PM_{2.5}$ (0.02) and AOD:$PM_{2.5}$ (0.01) ratios. The majority of the weight in the blended dataset is given to the kriging data, with moderate influence from WRF-Chem and Facebook data in a few locations. Facebook data receives little or no weight at most sites in the blended dataset because it is well correlated with the kriging data (R^2 = 0.43). In Figure 13 we show the correlation of the Facebook and kriging datasets at each surface site. In general, the two datasets are well correlated throughout the domain. The locations where the Facebook and kriging data disagree are in locations where neither dataset

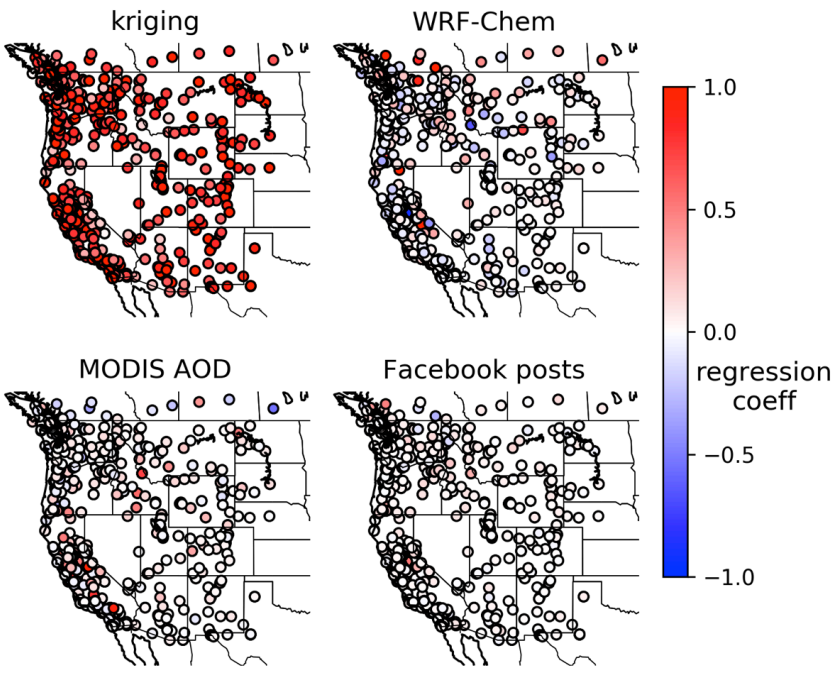

Figure 12: Regression coefficients given to each individual dataset at surface monitor locations in the GWR blend. Facebook and MODIS AOD regression coefficients have been normalized by the Facebook:$PM_{2.5}$ and AOD:$PM_{2.5}$ ratios empirically found with the data used in this study. These values are given in the main text. Note: these are the Facebook post weights without taking CF into account.

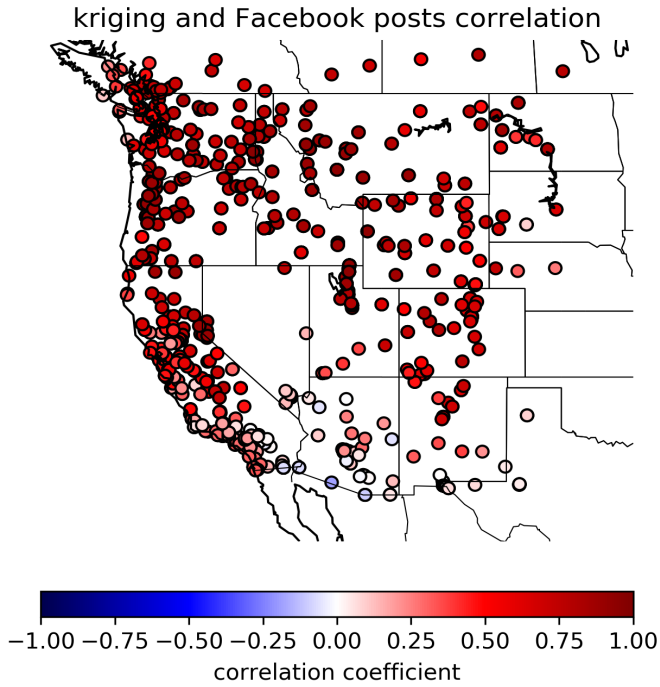

Figure 13: Correlation coefficient between the kriged surface monitors and Facebook posts at surface monitor locations. We use the leave-one-out cross validation kriging estimate in the calculation of the correlation coefficient.

accurately estimates $PM_{2.5}$ concentrations (namely, Arizona and southern New Mexico). While the strong agreement between Facebook posts and interpolated surface monitors is remarkable, the Facebook data does not provide sufficient new, orthogonal information to the blended dataset to significantly improve its performance.

4. CONCLUSIONS AND FUTURE WORK

In this work, we address two questions regarding the impact of wildfire smoke on air quality and public health in the western US. The first question asked, "*What fraction of summer $PM_{2.5}$ is attributable to wildfire smoke, and how is that fraction changing in fire-impacted regions as wildfire occurrence increases?*". To address this question we provide the first estimates of trends in fire-specific $PM_{2.5}$. We estimate these trends in fire-specific $PM_{2.5}$ with two distinct methods: 1) surface monitor observations combined satellite estimates of smoke influence and 2) the GEOS-Chem model with GFED4 biomass burning emissions.

Our updated record of US $PM_{2.5}$ trends show continuing improvements in air quality in the eastern US. We show that without the impact of wildfire smoke, these improvements would also be visible in the summer in much of the western US. We quantify the contribution of wildfire smoke to summer-mean $PM_{2.5}$ in the PNW region, heavily impacted by wildfires, over the past 11 years and find wildfire smoke contributes more than 50% of the summer-mean $PM_{2.5}$ in large fire years but with large interannual variability making trend assessment challenging. We hypothesize that smoke $PM_{2.5}$ trends may be significant in the western US if our method (which involves HMS that does not go back further than 2006) could be applied over a longer time period. As wildfires are expected to continue to increase in frequency and severity in the western US, we also hypothesize that our methods may be used to determine significant trends in smoke $PM_{2.5}$ in the future if monitor and HMS data sources operate continuously. This work adds to the current literature on US trends in $PM_{2.5}$ by attributing observed increases (and lack of significant trends) in PNW summer-average $PM_{2.5}$ to wildfire smoke.

Changes in air quality from wildfire smoke can have a significant impact on public health. Recent work has projected that by the end of the 21st century we may expect a doubling in premature deaths attributable to wildfire smoke in the US (Ford et al., 2018). In the future, we hope to perform a health impact assessment on our observation-based estimates of fire-specific $PM_{2.5}$ over the past decade. This will allow us to investigate if we can already observe these projected changes in the public health burden in the western US due to changes in wildfire smoke.

The second question we aimed to address in this work asked, "*Can we improve blended smoke-exposure estimates with the addition of user-generated information, and how do these blended exposure models perform across the entire western US?*". In response to this question, we developed two blended smoke-exposure models for the western US. The first model included: kriged surface observations, WRF-Chem simulations, and MODIS AOD; the second model included the previously mentioned input datasets as well as Facebook data. Overall, the blended smoke-exposure models perform well across most of the western US with an $R^2 = 0.66$, evaluated against surface observations. However, there is little difference in the performance of the blended exposure model with the addition of the Facebook data due to the strong correlation of the Facebook and kriged-surface-monitor data ($R^2 = 0.43$).

We acknowledge the performance of the individual datasets used in our blended model may differ by region in the US. Here we focus on the western US, which has historically been fractionally more impacted by wildfire smoke. However, large wildfires impacted the southeastern US in fall 2016, and the region is regularly impacted by smoke from prescribed

fires (Brey et al., exp2018). A recent future projection estimates that the southeastern US could be increasingly prone to wildfires over the next century (Ford et al., 2018) and there has already been research investigating the health impact of wildfire smoke using fires in the southeastern US (Rappold et al., 2011).

We believe the performance of smoke-exposure datasets may differ between the western and southeastern US. Examples of potential impacts on each dataset include: 1) Surface monitors: In the western US, where surface monitors are more sparse, an interpolation between monitors may have greater uncertainty than a similar interpolation in the SE US, where more monitors would feed the interpolation. 2) Satellite-derived AOD: Despite noted discrepancies between surface measurements and AOD in summer in the SE US, (e.g. Ford and Heald, 2013), MODIS AOD performance and AOD correlations with $PM_{2.5}$ are generally higher in the SE US compared to other US regions due to a more-spatially-consistent dark surface (Li et al., 2015; Sayer et al., 2014; Zhang et al., 2009). 3) CTMs: CTMs can have difficulty with the flow of smoke through complex topography in the western US and the greater variability of smoke injection heights in the western US [Val Martin et al., 2010]. These are just a few examples of factors that differ between the western and southeastern US, which may impact the performance of smoke estimation tools. In the future, we intend to investigate how these datasets (without the Facebook dataset) may perform across these two fire-impacted regions and determine the best tool for smoke-exposure estimates in each region.

BIBLIOGRAPHY

Abatzoglou, J. T., & Williams, A. P. (2016). Impact of anthropogenic climate change on wildfire across western US forests. *Proceedings of the National Academy of Sciences*, *113*(42), 11770–11775. https://doi.org/10.1073/pnas.1607171113

Abel, F., Hauff, C., Houben, G.-J., Stronkman, R., & Tao, K. (2012). Twitcident: Fighting Fire with Information from Social Web Streams. In *Proceedings of the 21st International Conference on World Wide Web* (pp. 305–308). New York, NY, USA: ACM. https://doi.org/10.1145/2187980.2188035

Alman, B. L., Pfister, G., Hao, H., Stowell, J., Hu, X., Liu, Y., & Strickland, M. J. (2016). The association of wildfire smoke with respiratory and cardiovascular emergency department visits in Colorado in 2012: a case crossover study. *Environmental Health*, *15*, 64. https://doi.org/10.1186/s12940-016-0146-8

Balch, J. K., Bradley, B. A., Abatzoglou, J. T., Nagy, R. C., Fusco, E. J., & Mahood, A. L. (2017). Human-started wildfires expand the fire niche across the United States. *Proceedings of the National Academy of Sciences*, *114*(11), 2946–2951. https://doi.org/10.1073/pnas.1617394114

Barbero, R., Abatzoglou, J. T., Larkin, S., Kolden, C. A., & Stocks, B. (2015). Climate change presents increased potential for very large fires in the contiguous United States. *International Journal of Wildland Fire*, *24*(7), 892–899. https://doi.org/10.1071/WF15083

Bedo, M., Blanco, G., Oliveira, W., Cazzolato, M., Costa, A., Rodrigues, J., et al. (2015). Techniques for effective and efficient fire detection from social media images. *ArXiv:1506.03844 [Cs]*. Retrieved from http://arxiv.org/abs/1506.03844

Blanchard, C. L., Hidy, G. M., Tanenbaum, S., Edgerton, E. S., & Hartsell, B. E. (2013). The Southeastern Aerosol Research and Characterization (SEARCH) study: Temporal trends in gas and PM concentrations and composition, 1999–2010. *Journal of the Air & Waste Management Association*, *63*(3), 247–259. https://doi.org/10.1080/10962247.2012.748523

Brey, S. J., Barnes, E., Pierce, J. R., & Fischer, E. V. (exp2018). Environmental conditions, ignition type, and air quality impacts of wildfires in the southeastern and western US. *In Review, AGU Earth's Future*.

Brey, S. J., Ruminski, M., Atwood, S. A., & Fischer, E. V. (2018). Connecting smoke plumes to sources using Hazard Mapping System (HMS) smoke and fire location data over North America. *Atmos. Chem. Phys.*, *18*(3), 1745–1761. https://doi.org/10.5194/acp-18-1745-2018

Chin, M., Rood, R. B., Lin, S.-J., Müller, J.-F., & Thompson, A. M. (2000). Atmospheric sulfur cycle simulated in the global model GOCART: Model description and global properties. *Journal of Geophysical Research: Atmospheres*, *105*(D20), 24671–24687. https://doi.org/10.1029/2000JD900384

De Longueville, B., Smith, R. S., & Luraschi, G. (2009). "OMG, from Here, I Can See the Flames!": A Use Case of Mining Location Based Social Networks to Acquire Spatio-temporal Data on Forest Fires. In *Proceedings of the 2009 International Workshop on*

Location Based Social Networks (pp. 73–80). New York, NY, USA: ACM. https://doi.org/10.1145/1629890.1629907

Dockery, D. W., Pope, C. A., Xu, X., Spengler, J. D., Ware, J. H., Fay, M. E., et al. (1993). An Association between Air Pollution and Mortality in Six U.S. Cities. *New England Journal of Medicine*, *329*(24), 1753–1759. https://doi.org/10.1056/NEJM199312093292401

van Donkelaar, A., Martin, R. V., Brauer, M., Kahn, R., Levy, R., Verduzco, C., & Villeneuve, P. J. (2010). Global Estimates of Ambient Fine Particulate Matter Concentrations from Satellite-Based Aerosol Optical Depth: Development and Application. *Environmental Health Perspectives*, *118*(6), 847–855. https://doi.org/10.1289/ehp.0901623

van Donkelaar, A., Martin, R. V., Levy, R. C., da Silva, A. M., Krzyzanowski, M., Chubarova, N. E., et al. (2011). Satellite-based estimates of ground-level fine particulate matter during extreme events: A case study of the Moscow fires in 2010. *Atmospheric Environment*, *45*(34), 6225–6232. https://doi.org/10.1016/j.atmosenv.2011.07.068

van Donkelaar, A., Martin, R. V., Spurr, R. J. D., & Burnett, R. T. (2015). High-Resolution Satellite-Derived PM2.5 from Optimal Estimation and Geographically Weighted Regression over North America. *Environmental Science & Technology*, *49*(17), 10482–10491. https://doi.org/10.1021/acs.est.5b02076

Efron, B. (1982). *The Jackknife, the Bootstrap and Other Resampling Plans*. Society for Industrial and Applied Mathematics.

Elliott, C. T., Henderson, S. B., & Wan, V. (2013). Time series analysis of fine particulate matter and asthma reliever dispensations in populations affected by forest fires. *Environmental Health*, *12*, 11. https://doi.org/10.1186/1476-069X-12-11

Emmons, L. K., Walters, S., Hess, P. G., Lamarque, J.-F., Pfister, G. G., Fillmore, D., et al. (2010). Description and evaluation of the Model for Ozone and Related chemical Tracers, version 4 (MOZART-4), *3*(1), 43–67. https://doi.org/10.5194/gmd-3-43-2010

Engel-Cox, Jill A., Holloman, Christopher H., Coutant, Basil W., and Hoff, Raymond M. (2004) Qualitative and quantitative evaluation of MODIS satellite sensor data for regional and urban scale air quality. *Atmospheric Environment, 38(16), 2495-2509. httpg://doi.org/10.1016/j.atmosenv.2004.01.039*

Ford, B., & Heald, C. L. (2013). Aerosol loading in the Southeastern United States: reconciling surface and satellite observations. *Atmos. Chem. Phys.*, *13*(18), 9269–9283. https://doi.org/10.5194/acp-13-9269-2013

Ford, B., Burke, M., Lassman, W., Pfister, G., & Pierce, J. R. (2017). Status update: is smoke on your mind? Using social media to assess smoke exposure. *Atmos. Chem. Phys.*, *17*(12), 7541–7554. https://doi.org/10.5194/acp-17-7541-2017

Ford, B., Martin, M. V., Zelasky, S. E., Fischer, E. V., Anenberg, S. C., Heald, C. L., & Pierce, J. R. (2018). Future Fire Impacts on Smoke Concentrations, Visibility, and Health in the Contiguous United States. *GeoHealth*, *0*(0). https://doi.org/10.1029/2018GH000144

Freitas, S. R., Longo, K. M., Chatfield, R., Latham, D., Dias, S., F, M. A., et al. (2007). Including the sub-grid scale plume rise of vegetation fires in low resolution atmospheric transport models. *Atmospheric Chemistry and Physics*, *7*(13), 3385–3398. https://doi.org/10.5194/acp-7-3385-2007

Gan, R. W., Ford, B., Lassman, W., Pfister, G., Vaidyanathan, A., Fischer, E., et al. (2017). Comparison of wildfire smoke estimation methods and associations with

cardiopulmonary-related hospital admissions. *GeoHealth*, *1*(3), 2017GH000073. https://doi.org/10.1002/2017GH000073

Gelaro, R., McCarty, W., Suárez, M. J., Todling, R., Molod, A., Takacs, L., et al. (2017). The Modern-Era Retrospective Analysis for Research and Applications, Version 2 (MERRA-2). *Journal of Climate*, *30*(14), 5419–5454. https://doi.org/10.1175/JCLI-D-16-0758.1

Giglio, Louis, Randerson James T., & Werf Guido R. (2013). Analysis of daily, monthly, and annual burned area using the fourth-generation global fire emissions database (GFED4). *Journal of Geophysical Research: Biogeosciences*, *118*(1), 317–328. https://doi.org/10.1002/jgrg.20042

Grell, G. A., Peckham, S. E., Schmitz, R., McKeen, S. A., Frost, G., Skamarock, W. C., & Eder, B. (2005). Fully coupled "online" chemistry within the WRF model. *Atmospheric Environment*, *39*(37), 6957–6975. https://doi.org/10.1016/j.atmosenv.2005.04.027

Guenther, A. B., Jiang, X., Heald, C. L., Sakulyanontvittaya, T., Duhl, T., Emmons, L. K., & Wang, X. (2012). The Model of Emissions of Gases and Aerosols from Nature version 2.1 (MEGAN2.1): an extended and updated framework for modeling biogenic emissions. *Copernicus*. Retrieved from http://dspace.mit.edu/handle/1721.1/78869

Hallar, A. G., Molotch, N. P., Hand, J. L., Livneh, B., McCubbin, I. B., Petersen, R., et al. (2017). Impacts of increasing aridity and wildfires on aerosol loading in the intermountain Western US. *Environmental Research Letters*, *12*(1), 014006. https://doi.org/10.1088/1748-9326/aa510a

Hand, J. L., Copeland, S. A., Day, D. E., Dillner, A. M., Indresand, H., Malm, W. C., et al. (2011). Spatial and Seasonal Patterns and Temporal Variability of Haze and its Constituents in the United States: Report V June 2011. Retrieved June 15, 2018, from

http://vista.cira.colostate.edu/Improve/spatial-and-seasonal-patterns-and-temporal-variability-of-haze-and-its-constituents-in-the-united-states-report-v-june-2011/

Hu, X.-M., Nielsen-Gammon, J. W., & Zhang, F. (2010). Evaluation of Three Planetary Boundary Layer Schemes in the WRF Model. *Journal of Applied Meteorology and Climatology*, *49*(9), 1831–1844. https://doi.org/10.1175/2010JAMC2432.1

Isaaks, E. H., & Srivastava, R. M. (1990). *An Introduction to Applied Geostatistics*. Oxford, New York: Oxford University Press.

Jaffe, D., Hafner, W., Chand, D., Westerling, A., & Spracklen, D. (2008). Interannual Variations in PM2.5 due to Wildfires in the Western United States. *Environmental Science & Technology*, *42*(8), 2812–2818. https://doi.org/10.1021/es702755v

Janssen, S., Dumont, G., Fierens, F., & Mensink, C. (2008). Spatial interpolation of air pollution measurements using CORINE land cover data. *Atmospheric Environment*, *42*(20), 4884–4903. https://doi.org/10.1016/j.atmosenv.2008.02.043

Kent, J. D., & Jr, H. T. C. (2013). Spatial patterns and demographic indicators of effective social media content during theHorsethief Canyon fire of 2012. *Cartography and Geographic Information Science*, *40*(2), 78–89. https://doi.org/10.1080/15230406.2013.776727

Lassman, W., Ford, B., Gan, R. W., Pfister, G., Magzamen, S., Fischer, E. V., & Pierce, J. R. (2017). Spatial and Temporal Estimates of Population Exposure to Wildfire Smoke during the Washington State 2012 Wildfire Season Using Blended Model, Satellite, and In-Situ Data. *GeoHealth*, 2017GH000049. https://doi.org/10.1002/2017GH000049

Leibensperger, E. M., Mickley, L. J., Jacob, D. J., Chen, W.-T., Seinfeld, J. H., Nenes, A., et al. (2012). Climatic effects of 1950–2050 changes in US anthropogenic aerosols – Part 1:

Aerosol trends and radiative forcing. *Atmos. Chem. Phys.*, *12*(7), 3333–3348. https://doi.org/10.5194/acp-12-3333-2012

Li, J., Carlson, B. E., & Lacis, A. A. (2015). How well do satellite AOD observations represent the spatial and temporal variability of PM2.5 concentration for the United States? *Atmospheric Environment*, *102*, 260–273. https://doi.org/10.1016/j.atmosenv.2014.12.010

Lindaas, J., Farmer, D. K., Pollack, I. B., Abeleira, A., Flocke, F., Roscioli, R., et al. (2017). Changes in ozone and precursors during two aged wildfire smoke events in the Colorado Front Range in summer 2015. *Atmospheric Chemistry and Physics*, *17*(17), 10691–10707. https://doi.org/10.5194/acp-17-10691-2017

Liu, J. C., Mickley, L. J., Sulprizio, M. P., Yue, X., Peng, R. D., Dominici, F., & Bell, M. L. (2016). Future respiratory hospital admissions from wildfire smoke under climate change in the Western US. *Environmental Research Letters*, *11*(12), 124018. https://doi.org/10.1088/1748-9326/11/12/124018

Luo, J., Du, P., Samat, A., Xia, J., Che, M., & Xue, Z. (2017). Spatiotemporal Pattern of $PM_{2.5}$ Concentrations in Mainland China and Analysis of Its Influencing Factors using Geographically Weighted Regression. *Scientific Reports*, *7*, 40607. https://doi.org/10.1038/srep40607

Malm, W. C., Schichtel, B. A., Hand, J. L., & Collett, J. L. (2017). Concurrent Temporal and Spatial Trends in Sulfate and Organic Mass Concentrations Measured in the IMPROVE Monitoring Program. *Journal of Geophysical Research: Atmospheres*, *122*(19), 2017JD026865. https://doi.org/10.1002/2017JD026865

McClure, C. D., & Jaffe, D. A. (2018). US particulate matter air quality improves except in wildfire-prone areas. *Proceedings of the National Academy of Sciences*, 201804353. https://doi.org/10.1073/pnas.1804353115

Murphy, D. M., Chow, J. C., Leibensperger, E. M., Malm, W. C., Pitchford, M., Schichtel, B. A., et al. (2011). Decreases in elemental carbon and fine particle mass in the United States. *Atmos. Chem. Phys.*, *11*(10), 4679–4686. https://doi.org/10.5194/acp-11-4679-2011

OECD. (2016). *The Economic Consequences of Outdoor Air Pollution*. Paris: Organisation for Economic Co-operation and Development. Retrieved from http://www.oecd-ilibrary.org/content/book/9789264257474-en

Olivier, J. G. J., Bouwman, A. F., Van der Maas, C. W. M., & Berdowski, J. J. M. (1995). Emission database for global atmospheric research (EDGAR): Version 2.0. In S. Zwerver, R. S. A. R. van Rompaey, M. T. J. Kok, & M. M. Berk (Eds.), *Studies in Environmental Science* (Vol. 65, pp. 651–659). Elsevier. https://doi.org/10.1016/S0166-1116(06)80262-1

Paglione, M., Saarikoski, S., Carbone, S., Hillamo, R., Facchini, M. C., Finessi, E., et al. (2014). Primary and secondary biomass burning aerosols determined by proton nuclear magnetic resonance (1H-NMR) spectroscopy during the 2008 EUCAARI campaign in the Po Valley (Italy). *Atmos. Chem. Phys.*, *14*(10), 5089–5110. https://doi.org/10.5194/acp-14-5089-2014

Pechony, O., & Shindell, D. T. (2010). Driving forces of global wildfires over the past millennium and the forthcoming century. *Proceedings of the National Academy of Sciences*, *107*(45), 19167–19170. https://doi.org/10.1073/pnas.1003669107

Rappold, A. G., Stone, S. L., Cascio, W. E., Neas, L. M., Kilaru, V. J., Carraway, M. S., et al. (2011). Peat Bog Wildfire Smoke Exposure in Rural North Carolina Is Associated with Cardiopulmonary Emergency Department Visits Assessed through Syndromic Surveillance. *Environmental Health Perspectives*, *119*(10), 1415–20. Retrieved from http://search.proquest.com/docview/900459812/abstract/9D5738DEB3854F07PQ/1

Reid, C. E., Brauer, M., Johnston, F. H., Jarrett, M., Balmes, J. R., & Elliott, C. T. (2016). Critical Review of Health Impacts of Wildfire Smoke Exposure. *Environmental Health Perspectives*, *124*(9), 1334–1343. https://doi.org/DOI:10.1289/ehp.1409277

Ridley, D. A., Heald, C. L., Ridley, K. J., & Kroll, J. H. (2018). Causes and consequences of decreasing atmospheric organic aerosol in the United States. *Proceedings of the National Academy of Sciences*, *115*(2), 290–295. https://doi.org/10.1073/pnas.1700387115

Rolph, G. D., Draxler, R. R., Stein, A. F., Taylor, A., Ruminski, M. G., Kondragunta, S., et al. (2009). Description and Verification of the NOAA Smoke Forecasting System: The 2007 Fire Season. *Weather and Forecasting*, *24*(2), 361–378. https://doi.org/10.1175/2008WAF2222165.1

Ruminski, M., Kondragunta, S., Draxler, R. R., & Zeng, J. (2006). *Recent Changes to the Hazard Mapping System*. Presented at the 15th Int. Emiss. Inventory Conf, (Reinventing Inventories). Retrieved from https://www.researchgate.net/publication/228625934_Recent_changes_to_the_Hazard_Mapping_System

Sachdeva, S., & McCaffrey, S. (2018). Using Social Media to Predict Air Pollution During California Wildfires. In *Proceedings of the 9th International Conference on Social Media*

and Society (pp. 365–369). New York, NY, USA: ACM. https://doi.org/10.1145/3217804.3217946

Sachdeva, S., McCaffrey, S., & Locke, D. (2017). Social media approaches to modeling wildfire smoke dispersion: spatiotemporal and social scientific investigations. *Information, Communication & Society*, *20*(8), 1146–1161. https://doi.org/10.1080/1369118X.2016.1218528

Sayer, A. M., Munchak, L. A., Hsu, N. C., Levy, R. C., Bettenhausen, C., & Jeong, M.-J. (2014). MODIS Collection 6 aerosol products: Comparison between Aqua's e-Deep Blue, Dark Target, and "merged" data sets, and usage recommendations. *Journal of Geophysical Research: Atmospheres*, *119*(24), 13,965-13,989. https://doi.org/10.1002/2014JD022453

Schichtel, B. A., Husar, R. B., Falke, S. R., & Wilson, W. E. (2001). Haze trends over the United States, 1980–1995 - ScienceDirect. *Atmospheric Environment*, *35*(30), 5205–5210. https://doi.org/10.1016/S1352-2310(01)00317-X

Song, W., Jia, H., Huang, J., & Zhang, Y. (2014). A satellite-based geographically weighted regression model for regional PM2.5 estimation over the Pearl River Delta region in China. *Remote Sensing of Environment*, *154*, 1–7. https://doi.org/10.1016/j.rse.2014.08.008

Spracklen, D. V., Mickley, L. J., Logan, J. A., Hudman, R. C., Yevich, R., Flannigan, M. D., & Westerling, A. L. (2009). Impacts of climate change from 2000 to 2050 on wildfire activity and carbonaceous aerosol concentrations in the western United States. *Journal of Geophysical Research: Atmospheres*, *114*(D20), D20301. https://doi.org/10.1029/2008JD010966

Spracklen, Dominick V., Logan, J. A., Mickley, L. J., Park, R. J., Yevich, R., Westerling, A. L., & Jaffe, D. A. (2007). Wildfires drive interannual variability of organic carbon aerosol in the western U.S. in summer. *Geophysical Research Letters*, *34*(16). https://doi.org/10.1029/2007GL030037

Thompson, G., Rasmussen, R. M., & Manning, K. (2004). Explicit Forecasts of Winter Precipitation Using an Improved Bulk Microphysics Scheme. Part I: Description and Sensitivity Analysis. *Monthly Weather Review*, *132*(2), 519–542. https://doi.org/10.1175/1520-0493(2004)132<0519:EFOWPU>2.0.CO;2

Travis, Katherine R., Jacob, Daniel J., Fisher, Jenny A., Kim, Patrick S., Marais, Eloise A. (2016). Why do models overestimate surface ozone in the Southeast United States? *Atmospheric Chemistry and Physics, 16(21),* 13561-13577. https://doi.org/10.5194/acp-16-13561-2016.

US EPA, O. (n.d.-a). 2011 National Emissions Inventory (NEI) Documentation [Policies and Guidance]. Retrieved January 31, 2017, from https://www.epa.gov/air-emissions-inventories/2011-national-emissions-inventory-nei-documentation

US EPA, O. (n.d.-b). Air Quality System (AQS) [Data and Tools]. Retrieved January 31, 2017, from https://www.epa.gov/aqs

Val Martin, M., Logan, J. A., Kahn, R. A., Leung, F. Y., Nelson, D. L., Diner, D. J. (2010). Smoke injection heights from fires in North America: analysis of 5 years of satellite observations. *Atmospheric Chemistry and Physics, 10(4),* 1491-1510. https://doi.org/10.5194/acp-10-1491-2010

Val Martin, M., Heald, C. L., Ford, B., Prenni, A. J., & Wiedinmyer, C. (2013). A decadal satellite analysis of the origins and impacts of smoke in Colorado. *Atmospheric Chemistry and Physics*, *13*(15), 7429–7439. https://doi.org/10.5194/acp-13-7429-2013

Val Martin, M., Heald, C. L., Lamarque, J. F., Tilmes, S., Emmons, L. K., & Schichtel, B. A. (2015). How emissions, climate, and land use change will impact mid-century air quality over the United States: A focus on effects at national parks. *Atmospheric Chemistry and Physics*, *15*, 2805–2823. Retrieved from http://dx.doi.org/10.5194/acp-15-2805-2015

van der Werf, G. R., Randerson, J. T., Giglio, L., Collatz, G. J., Mu, M., Kasibhatla, P. S., et al. (2010). Global fire emissions and the contribution of deforestation, savanna, forest, agricultural, and peat fires (1997–2009). *Atmos. Chem. Phys.*, *10*(23), 11707–11735. https://doi.org/10.5194/acp-10-11707-2010

Westerling, A. L., Hidalgo, H. G., Cayan, D. R., & Swetnam, T. W. (2006). Warming and Earlier Spring Increase Western U.S. Forest Wildfire Activity. *Science*, *313*(5789), 940–943. https://doi.org/10.1126/science.1128834

Westerling, Anthony LeRoy. (2016). Increasing western US forest wildfire activity: sensitivity to changes in the timing of spring. *Phil. Trans. R. Soc. B*, *371*(1696), 20150178. https://doi.org/10.1098/rstb.2015.0178

Wettstein, Z. S., Hoshiko, S., Fahimi, J., Harrison, R. J., Cascio, W. E., & Rappold, A. G. (2018). Cardiovascular and Cerebrovascular Emergency Department Visits Associated With Wildfire Smoke Exposure in California in 2015. *Journal of the American Heart Association*. Retrieved from https://www.ahajournals.org/doi/abs/10.1161/JAHA.117.007492

Wiedinmyer, C., Akagi, S. K., Yokelson, R. J., Emmons, L. K., Al-Saadi, J. A., Orlando, J. J., & Soja, A. J. (2011). The Fire INventory from NCAR (FINN): a high resolution global model to estimate the emissions from open burning. *Geoscientific Model Development; Katlenburg-Lindau*, *4*(3), 625. Retrieved from http://search.proquest.com/docview/1010614910/abstract/128EA229A2D4D97PQ/1

Xing, Y.-F., Xu, Y.-H., Shi, M.-H., & Lian, Y.-X. (2016). The impact of PM2.5 on the human respiratory system. *Journal of Thoracic Disease*, *8*(1), E69–E74. https://doi.org/10.3978/j.issn.2072-1439.2016.01.19

Yue, X., Mickley, L. J., Logan, J. A., & Kaplan, J. O. (2013). Ensemble projections of wildfire activity and carbonaceous aerosol concentrations over the western United States in the mid-21st century. *Atmospheric Environment*, *77*, 767–780. https://doi.org/10.1016/j.atmosenv.2013.06.003

Zhang, H., Hoff, R. M., & Engel-Cox, J. A. (2009). The Relation between Moderate Resolution Imaging Spectroradiometer (MODIS) Aerosol Optical Depth and PM2.5 over the United States: A Geographical Comparison by U.S. Environmental Protection Agency Regions. *Journal of the Air & Waste Management Association*, *59*(11), 1358–1369. https://doi.org/10.3155/1047-3289.59.11.1358

Zhu, L., Val Martin, M., Hecobian, A., Gatti, L. V., Kahn, R., & Fischer, E. V. (2018). Development and implementation of a new biomass burning emissions injection height scheme for the GEOSChem model. *Geoscientific Model Development Discussions*, 1–30. https://doi.org/10.5194/gmd-2018-93

APPENDIX

Alternative Statistical Approach for GEOS-Chem and Monitor-HMS Estimates of Trends

For the alternative statistical approach, we follow a similar methodology outlined in the main text with the exception of the linear-least squares regression and associated significance test. Here we estimate slopes using the Theil-Sen estimator (Theil, 1950), which calculates a linear least squares regression between each possible pair of points in the dataset (here, each available year) and takes the median of the resulting slopes. We use Kendall's tau to estimate the statistical significance of the correlation between years and concentrations at a 95% confidence level, with a null hypothesis of independence. The Theil-Sen estimator and Kendall's tau have been used recently in air quality trend studies (Hand et al., 2011; Malm et al., 2017) as they are less sensitive to outliers. We apply this alternative statistical approach to the datasets shown in Figures 1 and 2 of the main text. Results are presented in Figures 14 and 15. The two methods result in similar slopes for each dataset across the domain.

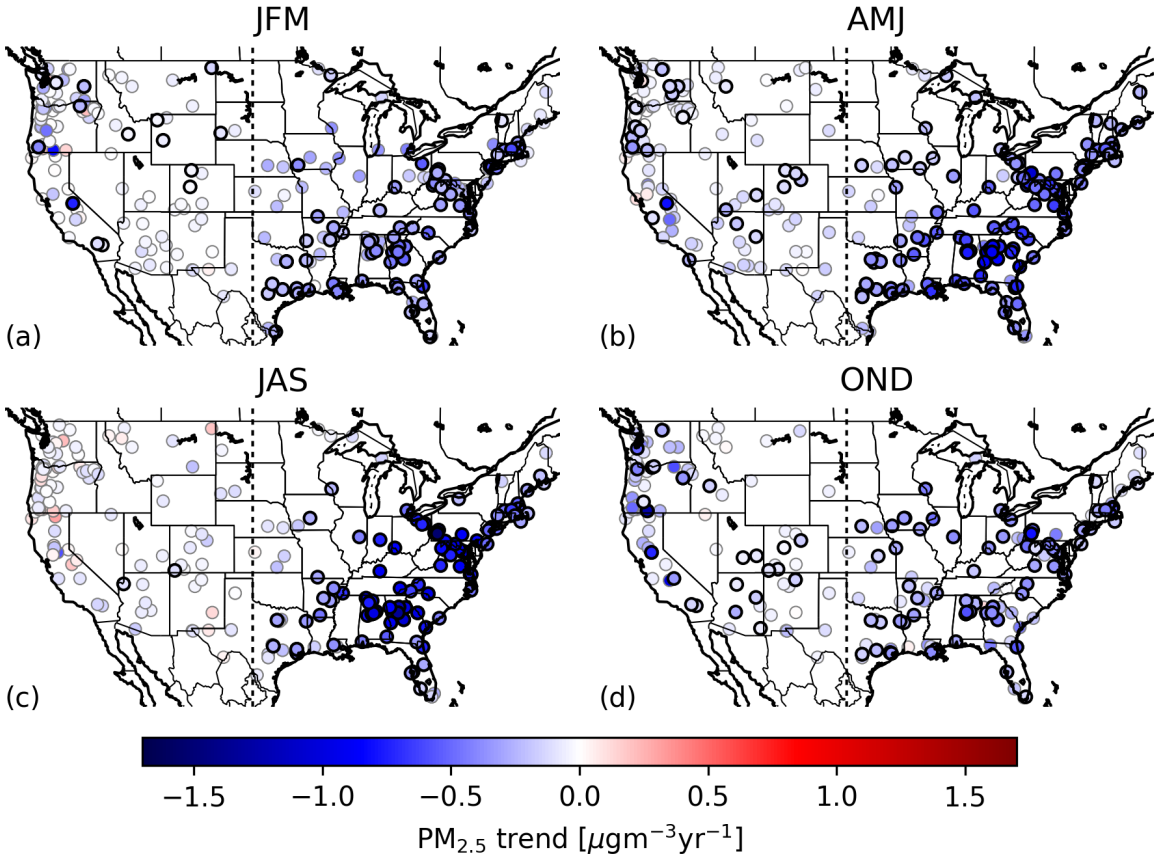

Figure 14 : Thiel slopes of seasonal-mean $PM_{2.5}$ at EPA AQS sites from 2006-2016. Sites with significant correlations at the 95% confidence level according to Kendall's tau are outlined in black; sites with insignificant correlations are outlined in gray. Dashed line shown at 100° W.

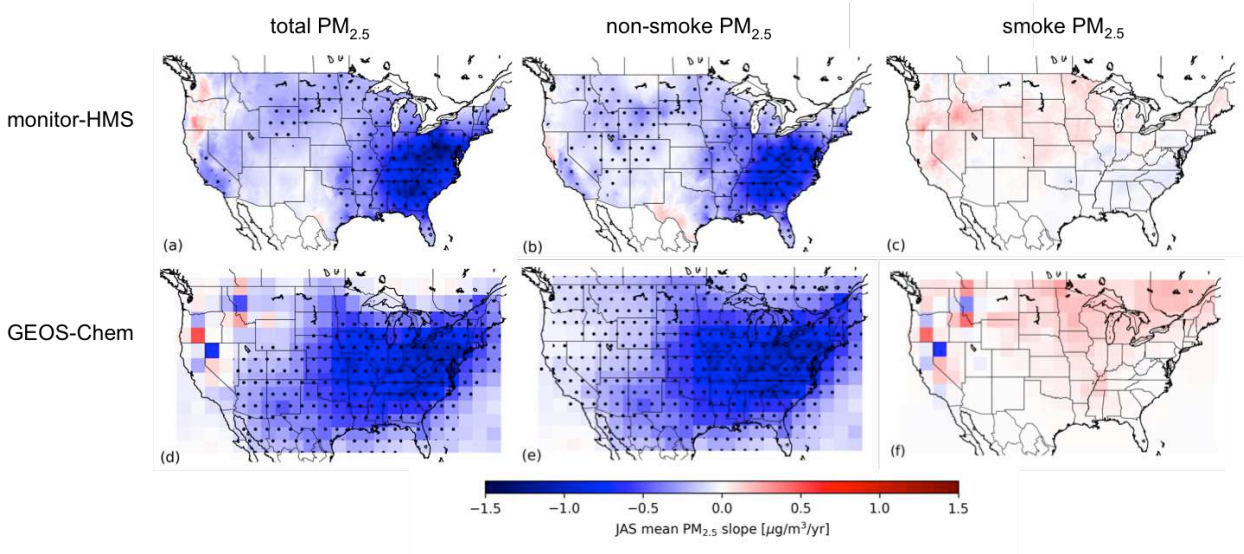

Figure 15: Thiel slopes of summer-mean (JAS) total $PM_{2.5}$, non-smoke $PM_{2.5}$, and smoke $PM_{2.5}$ from 2006-2016 for the monitor-HMS (panels a, b, and c) and GEOS-Chem (panels d, e, and f) methods. Locations with significant correlations at the 95% confidence level according to Kendall's tau are dotted.